Integrated torque sensor for e-bike motors

Björn Helander

Master's Thesis approved June 12, 2014
Public available February 3, 2015

LUNDS UNIVERSITET
Lunds Tekniska Högskola

Höganäs

Master's Thesis

Electrical Measurements

Faculty of Engineering, LTH
Department of Biomedical Engineering

Supervisor: Hans W. Persson

This project is the final work in the Master of Science in electrical engineering education at Lund's University. The education is given by the faculty of engineering and the project was supervised by the Department of Measurement Technology. This project has been a collaboration with Höganäs AB where the majority of the work has been performed. The project extended over five months and was started in January 2014. I would like to thank Höganäs AB for the opportunity to do my Master's Thesis at their company and for funding the project. I would like to thank Lars Sjöberg and David Johansson at Höganäs for their input and time. I especially want to thank my supervisor at Höganäs Cristofaro Pompermaier for sharing his knowledge with me and all his help with this project.

Abstract

Höganäs AB develops and build motors for e-bikes and with the current legislation the e-bikes must be equipped with a torque sensor to measure the torque applied by the rider. The motor may only assist when the rider pedals and there is no throttle on e-bikes. Höganäs want to develop a torque sensor that is integrated in the e-bike motor. Physical sensing principles for measuring torque on e-bikes are evaluated and the currently used sensors and the competitors' solutions are analyzed. Two types of torque sensor concepts are developed and evaluated with FEA (Finite Element Analysis). One of the concepts is realized in a prototype for evaluation. To further evaluate if the prototype concept is feasible the noise levels in Höganäs e-bike motor was measured to estimate how the sensor will be affected. The specifications for a torque sensor is established with demands and desirable properties for an integrated torque measurement system.

Contents

1 Introduction **1**
- 1.1 Background . . . 1
- 1.2 Purpose . . . 1
- 1.3 Delimitations . . . 2

2 Theory **3**
- 2.1 Physical Sensing principles . . . 3
  - 2.1.1 Strain gauge . . . 3
  - 2.1.2 Surface acoustic wave sensors . . . 5
  - 2.1.3 Multicore optical fiber sensor . . . 6
  - 2.1.4 LVDT-Linear variable differential transformer . . . 6
  - 2.1.5 Magnetostrictive sensing principle . . . 7
  - 2.1.6 Hall-effect . . . 8
  - 2.1.7 Piezoelectric effect . . . 10
  - 2.1.8 Measuring torsion . . . 11
  - 2.1.9 Measuring torsion with magnetic pattern . . . 11
  - 2.1.10 Measuring torque via a change in reluctance . . . 13
- 2.2 Theory for proposed sensors . . . 13
  - 2.2.1 Changing reluctance single magnet sensor . . . 13
  - 2.2.2 Dual magnet ring sensor . . . 14
  - 2.2.3 Using the torque sensor for index rotor position . . . 19
- 2.3 Demagnetization of NeFeB magnets . . . 20
- 2.4 Currently used sensors . . . 21
  - 2.4.1 ID bike TMM4 . . . 21
  - 2.4.2 Thun X-Cell RT . . . 21

3 Method **23**
- 3.1 Investigation of competitors' solutions . . . 23
- 3.2 FEA of magnetic based torque sensors . . . 23
  - 3.2.1 CAD-model of sensor . . . 23
  - 3.2.2 Meshing the model . . . 23
  - 3.2.3 Defining boundary conditions . . . 24
  - 3.2.4 Extracting results . . . 24
- 3.3 Simulink models of sensor . . . 24

3.4 Prototype of torque sensor 24
3.4.1 Measuring magnetic flux density in Höganäs motor 26

4 Results **27**
4.1 Competitors' solutions 27
4.1.1 BionX torque sensor 27
4.1.2 GO SwissDrive torque sensor 27
4.1.3 Xion motor torque sensor 32
4.2 Specifications torque sensor 34
4.3 Changing reluctance single magnet sensor 35
4.3.1 FEA simulation of the magnetic circuit 35
4.3.2 FEA simulation of the prototype 35
4.3.3 Prototype result 38
4.4 Dual magnet ring sensor 43
4.4.1 Sensitivity to geometrical errors 44

5 Discussion **45**
5.1 Limitations due to patents 45
5.1.1 Patent No. CA 2,426,109 45
5.1.2 Patent No. US 4,784,002 45
5.1.3 Patent No. US 6,598,490 45
5.2 Evaluated torque sensors 46
5.2.1 Changing reluctance single magnet sensor 46
5.2.2 Dual magnet rings 46
5.3 Future goals 47

6 Bibliography **49**

Appendix A Drawings for sensor prototype **51**

Appendix B Simulink model for dual magnet ring sensor **57**

1 Introduction

1.1 Background

Höganäs AB is one of the world's leading manufacturer of metal powders and one of the products Somaloy is a metal powder specially designed for electromagnetic applications (e.g. electric motors, inductors etc.) machines. The metal powder is covered with a thin non-organic coating to make it electrically isolated. This isolation prevents eddy currents making it ideal for electric machines. For many years Höganäs have helped its customers in developing electric machines with Somaloy and in the process acquired know how in electric machines and Höganäs started developing an electric motor specially designed for Electrically Power Assisted Cycle (EPAC) or e-bikes.

With the current legislation for e-bikes the electric motor may only assist the rider when the rider pedals. The motor has no throttle to control how much power it should supply and the torque output is proportional to the torque supplied by the rider. This pedal torque needs to be measured to control the motor in a satisfactory way. In the current design Höganäs relies on sensors developed by third party companies and these sensors are not integrated in the motor. There are a number of advantages if the torque sensor is integrated in the motor for example the number of cables needed when installing the motor will decrease, the number of total components that you need to install on the bike decrease. The overall robustness of the system will also increase since there will be less risk for cable breakage and the cost is reduced. But moving the sensor into the motor introduces a number of new problems for example that you need to transfer the signal from the motor to the motor control unit, you have higher ambient temperature for the sensor and cables with high current in the proximity. You also have limited space and must consider redesigning the rest of the motor.

1.2 Purpose

The purpose of this project is summarized in the following list:

- Contribute with information and ideas towards a permanent torque measurement solution for Höganäs E-bikes that is integrated in the motor.

- Make a specification on requirements and desirable properties for a torque measuring system integrated in an e-bike motor.
- Investigate current patents for integrated torque sensors and what consequences they have for Höganäs development of an integrated torque sensor.
- Study the sensors currently used with the e-bike motor as well as sensors used by competitors.
- Gather information on possible physical sensing principals that can be used for sensing torque in an e-bike motor.
- FEA analysis of selected torque sensors.
- Design and evaluate a prototype sensor.

1.3 Delimitations

The evaluation of sensor solutions for measuring torque will not be performed on a real E-bike. The evaluation will consist of simulations, theoretical analysis and evaluation of a prototype sensor in a lab environment. The argument for not testing the sensor in a real system is that it is not feasible to complete it within the time limit for this project.

2 Theory

2.1 Physical Sensing principles

This chapter will give a theoretical background for different types of physical sensing principles. The different sensing principles are often suited to measure more than one type of physical quantities for example force and torque depending on how the sensor is mounted and configured.

Torque is hard to measure directly, and often we measure a different physical quantity that changes when we apply torque. A classic example of this is to measure torsion of an axle since the torsion is proportional to the applied torque. Another way of measuring torque is to measure strain in a material, for example when torque is applied to an axle it is possible with strain gauges to measure the strain in the axle and relate this to the applied torque.

The different techniques all have different advantages for example:

- Temperature dependencies
- Might require advanced electronics to acquire a good signal
- Different noise sensitivity
- Sensitive to mechanical disturbance
- Sensitive to mechanical tolerances

When measuring the torque applied by the rider of the bike it is important that the torque applied by the motor does not interfere with the measurement. It is also important that the measurement is insensitive to external forces for example if the rider sits down hard in the saddle or if the rider drives over an obstacle on the road. These external forces produce a strain on the back axle that is vertical, whereas the torque applied by the rider produces a strain in the horizontal plane.

2.1.1 Strain gauge

The strain gauge is one of the most common sensors for converting a physical quantity to an measurable electric quantity. The basic principle for the strain gauge is the increase in resistance that occurs when a wire is stretched due to

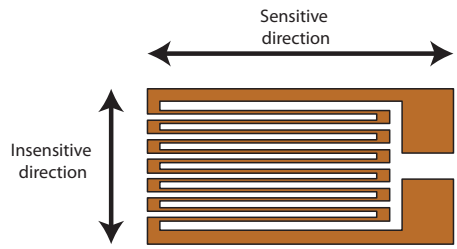

Figure 2.1: The basic design of a metal foil strain gauge

strain. By arranging the wire to have a large length in one direction and short length in the perpendicular direction we get a sensor that is sensitive to strain in only one direction. The basic design of a strain gauge is illustrated in Figure 2.1. The relative change in resistance $\frac{\Delta R}{R}$ for a metal foil strain gauge is described by [1]

$$\frac{\Delta R}{R} = \frac{\Delta \rho}{\rho} + (1 + 2\gamma) \cdot \frac{\Delta L}{L} \tag{2.1}$$

where ρ is the resistivity of the material used, L is the length of the wire and γ is the Poisson number which relates the strain and change in cross sectional area. To be able to compare different types of strain gauges we use the gauge factor defined as [2]

$$k = \frac{\frac{\Delta R}{R}}{\frac{\Delta L}{L}} \tag{2.2}$$

The gauge factor is typically in the range of 2-4 for metal foil strain gauges, and as large as 200 for semi-conductor based strain gauges[2]. This large difference in gauge factor is due the change in resistance in metal foil is only dependent on the geometric change whereas in silicon based strain gauges the change is mostly due to the piezoresistive effect [3]. For piezoresistive materials the resistivity changes when stress is applied to them.

The change in resistance is in the range of 0.001%-1% and is hard to measure. To transform the problem from measuring a small change in resistance to measure a change in voltage the strain gauge is often connected in a connection bridge see Figure 2.2 which illustrates the Wheatstone bridge. The bridge produces a voltage proportional to the strain and is easily amplified. Other types of bridge configurations are also possible. Strain gauges made from metal foil is glued on the material in which the strain is to be measured, and the orientation of the strain gauge is important since it only measures in one direction. For silicon sensors the strain sensor is often incorporated in some larger structure

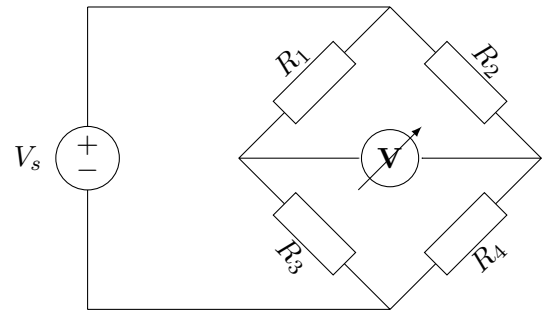

Figure 2.2: Strain gauges in a Wheatstone bridge

by doping conductive lines in the silicon. Since the resistance of a material is dependent on the temperature the strain gauge is temperature sensitive. This can be circumvented in the Wheatstone bridge by placing all the resistors (R1 to R4) at the same location then they are all equally affected by the change in temperature. Figure 2.3 illustrates the use strain gauges for measuring the bend of the back axle caused by the applied torque. In the illustration both horizontal and vertical bending is measured.

2.1.2 Surface acoustic wave sensors

Surface acoustic wave (SAW) sensors can be used as the strain gauges to measure strain. The sensor utilizes sound waves traveling along a surface to sense changes in the structure of the surface. There are two types of SAW sensors, the resonating sensors and delay line sensors [4]. In resonating sensors the sensor is excited with a wave and the resonating structure will resonate at a specific frequency. The resonating structure will be affected if the sensor is strained. For delay lines there are two or more reflectors at different distance from the antenna. When a wave travels along the sensor it will be reflected and depending on the distance between the antenna and the reflectors there will be a time difference between the reflections that depends on the distance between the reflectors and in turn the strain in the sensor.

The SAW sensor is resilient to disturbances since it utilizes sound waves, for example the sensors are immune to magnetic and electric fields, but the sensor is sensitive to changes in temperature since it will change the length of the sensor.

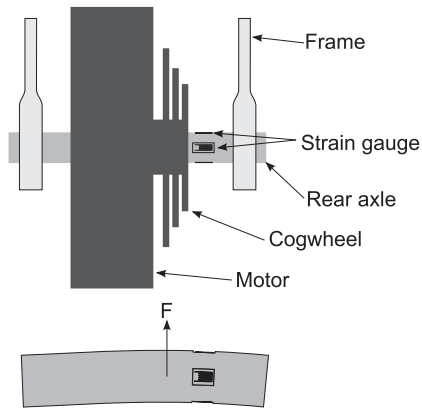

Figure 2.3: Measuring the bend of the rear axle with strain gauges to determine the applied torque.

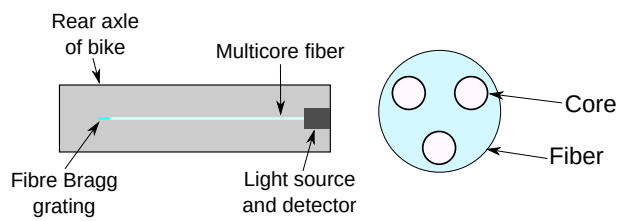

Figure 2.4: Measuring bend on rear axle with a multicore optical fiber.

2.1.3 Multicore optical fiber sensor

Optical fibers with multiple cores can be used for detecting bending in two directions [5]. When the fibers bends the path length for the for individual cores changes and when the light reach the detector at one end of the fiber there is a phase-shift since the light has traveled different lengths in the cores. This phase difference will create a diffraction pattern that is related to how much the fiber has been bent. Figure 2.4 illustrates how multicore optical fibers can be used to measure the bend of the rear axle of an e-bike.

2.1.4 LVDT-Linear variable differential transformer

A sensor used to measure linear distances accurately is the Linear Variable Differential Transformer (LVDT). The LVDT consist of three windings around

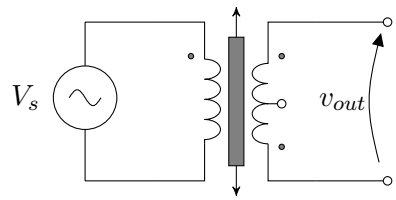

Figure 2.5: Schematic design for the LVDT

a movable core. There is one primary and two secondary windings with opposite phase. When the core moves the magnetic coupling between the primary and the two secondary windings change, see Figure 2.5. This is the mechanism that generates a signal correlated to the movement of the core in the transformer. The generated signal has a linear relationship to the moved distance and the range for this sensor type is between $\pm 100\,\mu m$ to $\pm 25\,cm$ [6]. The supply voltage V_s is the typically between $1\,V_{RMS}$ to $24\,V_{RMS}$ and at frequencies ranging from $50\,Hz$ to $20\,kHz$ [6].

Figure 2.6 show a principal solution for measuring torque on an E-bike with the use of LDVT. By drilling a hole in the back axis and inserting a long pin and attach the tip a LVDT sensor, it might be possible to get a measure on how much the axle has been bent. Since the axle is rigid at the ends where it is attached to the frame it will only bend in the section that is in between the frame of the bike. Since the pin is held by the end of the axle it should not be affected by the force from the pedals. The distance between the pin and the LVDT-sensor changes as the axle is bent, giving a measurement on how much torque the rider applies. The magnitude of the bend of the rear axle is not known an has to be simulated or experimentally tested to see if it is feasible to measure the bending with LVDT-sensors or as described in Section 2.1.6 with Hall-sensors.

2.1.5 Magnetostrictive sensing principle

Magnetostrictive sensors use the magnetoelastic properties of a material to sense a physical property. Magnetostrictive materials have the ability to convert physical energy to magnetic energy and the other way around. If a magnetostrictive material is subjugated to mechanical strain or stress the magnetic properties of the material will change. It is possible to measure the change of the magnetic properties and get a reading on how the physical properties have changed. The relationship between strain ε , stress σ , Young´s modulus at constant magnetic

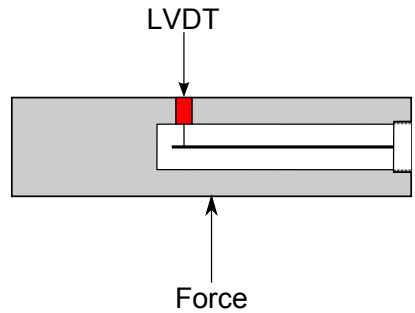

Figure 2.6: Measuring bending of the rear axle with LDVT

field E_y^H, applied magnetic field H, magnetic induction B and permeability at constant stress μ^σ is described by [7]

$$\varepsilon = \frac{\sigma}{E_y^H} + dH \tag{2.3}$$

$$B = d^*\sigma + \mu^\sigma H \tag{2.4}$$

where $d = \partial\varepsilon/\partial H|_\sigma$ and $d^* = \partial B/\partial\sigma|_H$ are the two magnetomechanical coefficients. Equation 2.4 stipulates that the magnetic induction is changed when a strain is applied to the material. By measuring B and H we can get a reading on how much strain we apply to the material. With magnetostrictive sensors it is possible to measure [7] for example force, torque, vibrations and flow rates depending on how the sensor is configured.

2.1.6 Hall-effect

When current flows through a semiconductor and an magnetic field is applied perpendicular to the current a small voltage (Hall-voltage) arises in the semiconductor see Figure 2.8. The Hall-voltage is perpendicular to both the direction of the current and the magnetic field. The Hall-voltage arise since the magnetic field will exert a force on moving charges. This force will give a higher concentration of electrons on one side of the material giving a small voltage. The difference in electron concentration will also give an electric field that counteracts the force generated by the magnetic field and the two forces will form an equilibrium. The resulting Hall-voltage is described by [8]

$$V_H = \frac{IB}{q_0 N d} \tag{2.5}$$

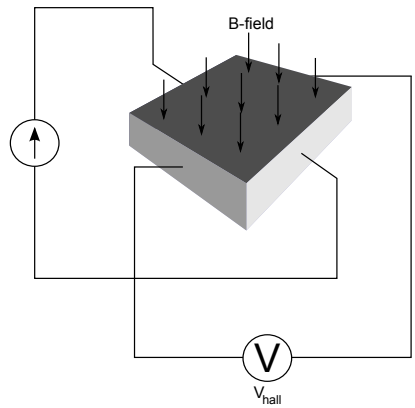

Figure 2.7: The principle of the Hall-effect.

where d is the thickness of the semiconductor, I is the current through the semiconductor, B is the magnetic field through the conductor, q_0 is the elementary charge and N is the charge carrier density in the semiconductor.

The Hall-effect is used in Hall-sensors to measure magnetic flux density since the resulting voltage is linearly dependent on the magnetic flux density. The resistance of the semiconductor is temperature dependent and to minimize the effect of varying temperature the current needs to be kept constant. If the current is kept constant the variations in the sensitivity of the Hall-sensor are minimized [8]. The Hall-sensor also have a temperature affected offset which may interfere with measurements when temperature changes. For a Hall-sensor IC with 0 V to 5 V output and with output 2.5 V when no B-field is applied the max sensitivity that can be used for a specific max B-field is then described by

$$S = \frac{V_{outMax} - V_{outZero}}{B_{max}} = \frac{5\,\mathrm{V} - 2.5\,\mathrm{V}}{B_{max}} = \frac{2.5\,\mathrm{V}}{B_{max}} \tag{2.6}$$

where V_{outMax} is the max voltage from the Hall-sensor, $V_{outZero}$ is the voltage when no B-field is applied and B_{max} is the highest strength of the B-field that you want to measure.

Figure 2.8 show a principal solution for measuring torque on an E-bike with the help of Hall-sensors. The technique works like the principle described in Section 2.1.4 but with a Hall-sensor instead of a LVDT senor. This requires a magnet on the tip of the needle and either the tip could be magnetized or a magnet could be attached to the pin.

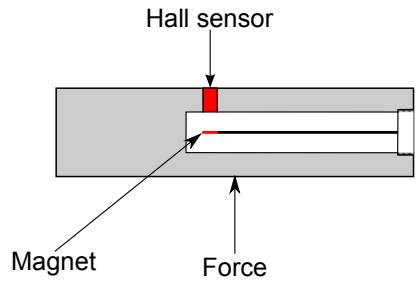

Figure 2.8: Measuring applied force on the rear axle with a Hall-sensor.

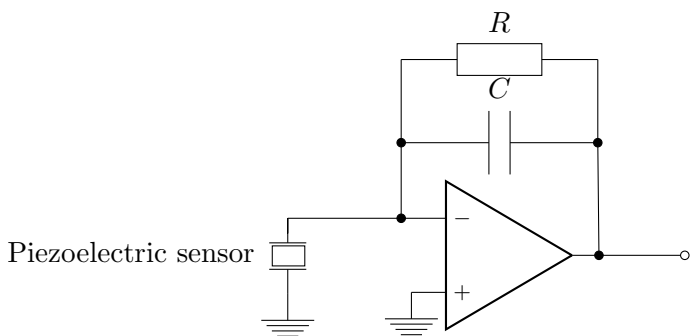

Figure 2.9: Schematic design for a Piezoelectric sensor circuit [1].

2.1.7 Piezoelectric effect

A piezoelectric material is a material that when exerted to a force produces a change in charge distribution resulting in a voltage over the material. The generated charge is related to the strain in the material [1]. The charge in the piezoelectric material will dissipate over time [1] and the sensor will eventually show zero for a static force and since the readout will change for static signals it is not suitable for static load, but for dynamic forces the piezoelectric material constantly generates a new charge. To measure the charge the piezoelectric material is connected to a charge amplifier. This type of amplifier has a capacitive feedback network. The charge from the piezoelectric material will charge the capacitor if the feedback network resulting in a measurable output voltage from the amplifier. In Figure 2.9 the basic design for a charge amplifier is illustrated.

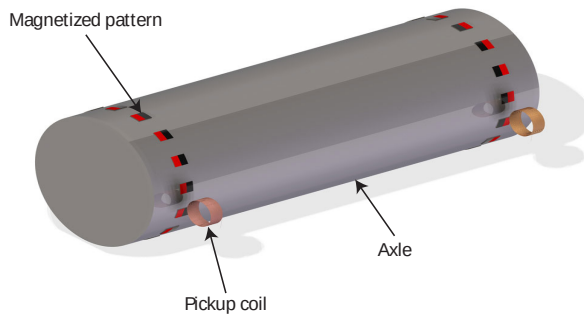

Figure 2.10: Measuring torque with magnetized pattern.

2.1.8 Measuring torsion

When torque is applied to an axle that is rigid in the other end it will cause torsion of the axle. The magnitude of the torsion is related to the applied torque and if the torsion is measured the torque can be calculated. The relationship between torque and torsion depends on the material of the axle and the shape of the axle and is described by [1]

$$M = \frac{G \cdot I\phi}{L} \tag{2.7}$$

where M is the applied torque, G is the shear modulus, ϕ is the twisting angle, L is the length of the axle and I is the torsion constant and is for a circular axle with radius a given by

$$I = \frac{\pi \cdot a^4}{2} \tag{2.8}$$

2.1.9 Measuring torsion with magnetic pattern

The technique described in Section 2.1.8 also works with magnetics. The axle is magnetized with a well-defined pattern consisting of several dipoles. The pattern is magnetized on two places along the axle, see Figure 2.10. When torque is applied to the axle it will cause torsion of the axle, and give a relative rotation of the magnetic patterns. By placing a pickup coil or a Hall-sensor next to each magnetic pattern a voltage is generated each time a magnetic dipole passes the coil. By comparing when the pulse arises in the two coils we get a small difference in phase or time. This phase difference is proportional to the torsion and in turn to the applied torque.

When magnetizing the pattern on the axle it is important that the magnets are correctly located. If the magnetic pattern is rotated slightly we will get a

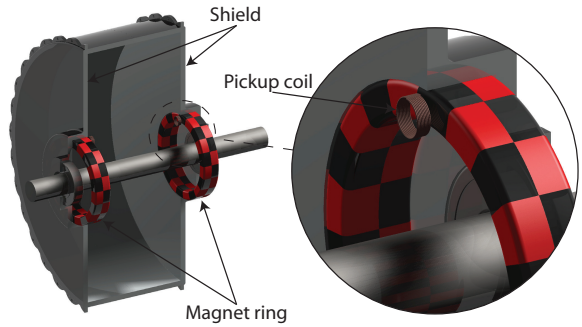

Figure 2.11: Measuring torque on non rotating axle with magnetized pattern.

phase difference even if there is no torsion of the axle. This phase difference could be compensated by calibrating the sensor such that the phase difference with no applied torque equals zero torque. The placement of the pickup coils will give the same effect and the sensor needs a zero level calibration. If we instead have a difference in magnet size we will get an error when we measure from that magnet and this error will only occur when the wrongly placed magnet passes the pickup coil.

This type of torque sensor is suitable for measuring torque when we have an rotating axle and works fine when the sensor is located in the bottom bracket. But if the sensor is located inside the motor we have no rotating axle to magnetize, but a section of the shields of the motor could be magnetized see Figure 2.11, and when torque is applied by the rider it will affect the shield on the side of the motor where the cog wheel is attached giving a torsion in the shield.

Since the shields of the motor is not one part it is problematic to get high precision when assembling the parts and it is hard to ensure that the magnetized patterns are located correctly. When magnetizing an axle it is easier to ensure that the magnetized patterns are correct since the axle is one solid piece. To avoid this problem the shield can be altered and two patterns are magnetized on the same side of the motor. The shield need to be altered so that we get a torsion between the two magnetized patterns The above described techniques for measuring torque by measuring torsion all have the disadvantage that you need rotation to measure the applied torque. If the motor is not rotating it does not matter how much torque the rider apply the sensor will still output zero torque. The sensor will get a reading of the torque first when the wheel has started turning and the motor will not start immediately when the rider applies torque.

2.1.10 Measuring torque via a change in reluctance

It is possible to measure torque by measuring a change in magnetic flux density. To get a change in magnetic flux density the reluctance needs to be changed in the magnetic circuit. The reluctance is the equivalent of resistance in an electric circuit. To change the reluctance you can insert or remove iron into the circuit. An air-gap in the circuit have much lower permeability than the same geometry with iron and by changing the width of an air-gap the reluctance in a magnetic circuit will change and in turn change the magnetic flux density. If the width of the air-gap depends on for example torque then the magnetic flux density will also depend on torque. The geometry of the sensor can be adapted to suit the application and the structure that change the reluctance need to be adopted to fit the physical quantity that you want to measure. The magnetic flux density needs to be measured to get a reading of the torque and since the magnetic flux is DC a Hall-sensor is a good candidate. The Hall sensor gives an output voltage as described in Section 2.1.6. The output from the Hall-sensor is temperature sensitive but in Hall-sensors ICs there are built in temperature compensation. The magnet used in the sensor is also temperature sensitive and will affect the measurements. An advantage of this sensor type is that it is possible to measure torque on a rotating structure, like in an e-bike motor.

2.2 Theory for proposed sensors

2.2.1 Changing reluctance single magnet sensor

One of the most challenging problems when designing a torque sensor for an e-bike motor is that you want to measure torque applied to a rotating structure but you want to have a sensor that stands still. The torque that the rider applies affects the hub of the motor and deforms the hub slightly but this is hard to measure. Another approach is to modify the hub to get a flexible coupling between the freewheel hub and the motor. This will transform the applied torque into a relative rotation between two parts of the hub. This basic idea is used in the e-bike motor Xion manufactured by Neodrives and the motor manufactured by GO SwissDrive AG see Section 4.1.2 and Section 4.1.3 for more information on the function of these torque sensors. This relative rotation is still hard to measure, either you measure the absolute position of both parts and calculate the relative rotation or you build a structure that is circular symmetric and has a change in a physical quantity that depends on the relative rotation.

In this sensor a single magnet ring is used with magnetization direction through the thickness of the magnet. The magnet ring is surrounded by an iron

structure that gives a reluctance that varies as the relative rotation is changed. The iron structure also forms a small air gap where the magnetic flux density can be measured. The air gap is circular symmetric and the sensor measuring the magnetic flux density travels along this gap as the motor turns. The air gap will have the same magnetic flux density the whole revolution of the motor and the magnetic flux density will only change if the relative rotation is changed. In Figure 2.12 the general principle for the changing reluctance sensor with a single magnet ring is illustrated.

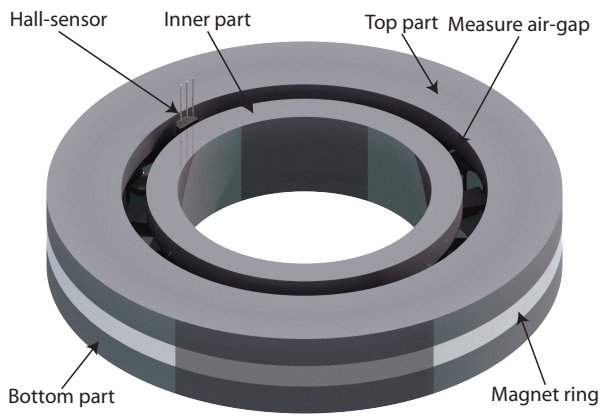

Figure 2.12: Torque sensor with a single magnet ring and changing reluctance.

The change in reluctance is achieved by a set of protruding teeth on the inner and bottom part of the sensor. The number of teeth is the same on both parts. When the teeth are aligned and facing each other we get low reluctance between the inner and outer part. When we have a relative rotation between the two parts and the teeth are not facing each other we get higher reluctance since the air gap between the teeth is larger. The variation of reluctance will affect the magnetic flux density in the measure air gap, and in turn the output signal from a Hall-sensor placed in the measure air gap. The reluctance changing motion is illustrated in Figure 2.13.

2.2.2 Dual magnet ring sensor

The technique described in Section 2.2.1 relies on a rather complicated structure to get a change in magnetic field density that depends on the applied torque. An alternative to this solution is to have two multipole magnets with different diameters see Figure 2.14. The smaller of the two magnets are situated concentric inside the larger magnet. Both of the magnets rotate along with the

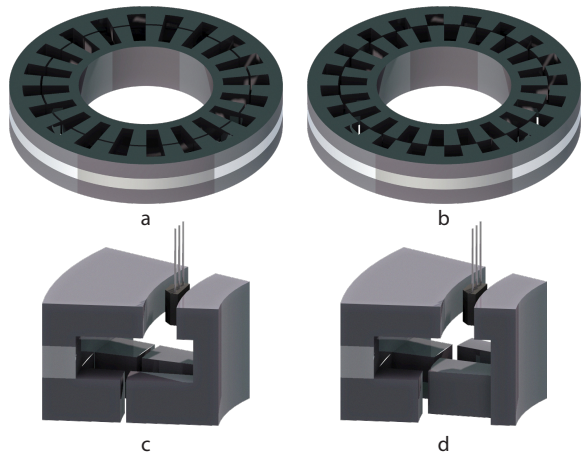

Figure 2.13: Reluctance change in the torque sensor.

shield of the motor but one of them is attached to a device that turns as torque is applied by the bicycle rider. This will cause a relative rotation between the two magnets that is related to the applied torque henceforth referred to as θ_{rel} and in Figure 2.15 the rotation is illustrated. The magnet rings has the same number of poles and the poles are in alternating direction. The direction is either towards the center of the magnet rings or outward from the center. The magnetic field density in the gap is then measured with a Hall-sensor and the Hall-sensor only measures the flux density that is perpendicular to the sensor. The sensor is oriented so that it measures magnetic flux density in the radial

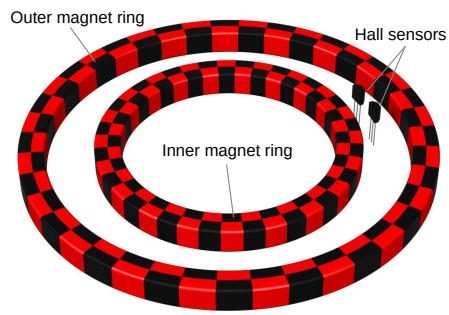

Figure 2.14: The basic concept of a torque sensor based on two multiple poles magnet rings.

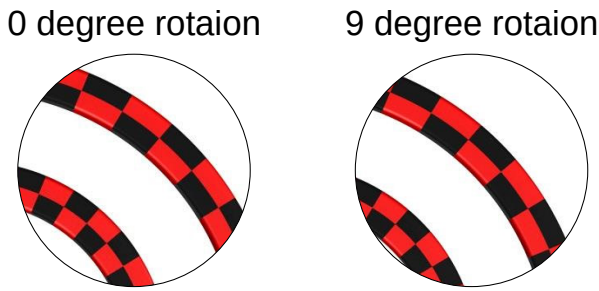

Figure 2.15: The magnetic rings when no torque is applied (left) and when max torque is applied (right).

direction (direction pointing towards the center of the magnets). Since the Hall-sensor will not rotate with the magnet rings it will measure is varying magnetic flux density depending on the current position of the sensor. To investigate how the magnetic flux density varies in the air gap the sensor was simulated in a FEA program. The dimensions used for the simulation are listed in Table 2.1 and the magnetic flux density is simulated in the center of the air gap between the two magnets.

Parameter	Value
Outer diameter large magnet	100 mm
Inner diameter large magnet	88 mm
Outer diameter small magnet	76 mm
Inner diameter small magnet	64 mm
Thickness of magnets	4 mm
Material of magnets	Hitachi/Nd-Fe-B NMX-S52
Number of magnetic poles	40 (20 in each direction)
Temperature	20 °C
Relative rotation θ_{rel}	0° to 9°

Table 2.1: Parameters used for FEA simulation of the sensor.

FEA simulations of this setup show that the signal will be a sinusoidal with frequency that is the number of magnetic pole pairs multiplied by the frequency of the motor. The simulation also show that the signal will also contain a harmonic with three times higher frequency and low amplitude compared to the first harmonic see Figure 2.16. The signal from the Hall-sensor is called S_{Hall1}

and is described by

$$S_{Hall1} = A \cdot \sin(\omega t) + B \cdot \sin(3\omega t + \phi) \tag{2.9}$$

where A is the amplitude of the first harmonic, B is the amplitude of the third harmonic, ω is the angular frequency of the signal and ϕ is the phase difference between the first and third harmonic.

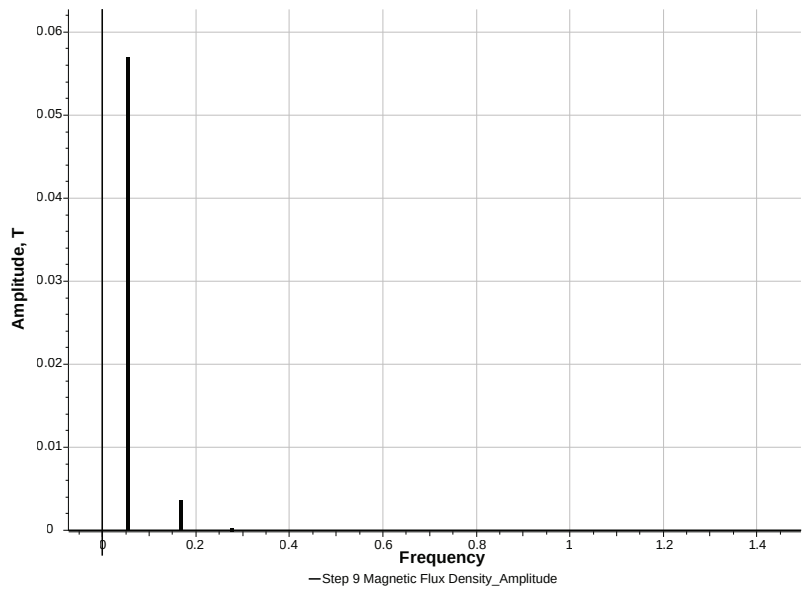

Figure 2.16: Frequency contents of the simulated magnetic flux density between two multipole magnets. The first harmonic is the frequency of the motor.

When θ_{rel} is zero we have the magnets aligned so that the poles in the inward direction are facing each other, and the same applies to the poles in the outward direction. This will give a high magnetic flux density in the air gap in the radial direction resulting in a large amplitude for S_{Hall1}. Note that the actual value of the signal at a specific time depends on how much the magnet has rotated and the amplitude is not known. When θ_{rel} is increased (the applied torque is increased) the alignment of the magnets change, and we get a lower magnetic flux density in the radial direction, see Figure 2.17 where the magnetic flux density is plotted for different values for θ_{rel}. From the plot it is clear that we also get a phase shift of the signal that is dependent on θ_{rel}.

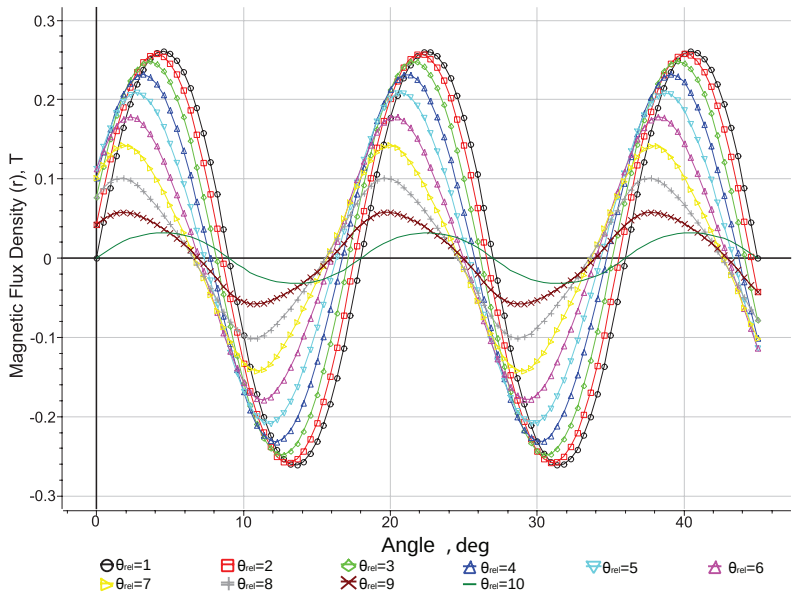

Figure 2.17: Magnetic flux density between two multipole magnets at different rotation angles θ_{rel}.

With one Hall-sensor we only get the instantaneous value and not the amplitude of the signal, this is a problem since it is the amplitude that is proportional to the applied torque. To get the amplitude one can use a second Hall-sensor placed such that it measures the signal with a 90° or $\pi/2$ rad shift. The signal from the phase shifted Hall-sensor is called S_{Hall2} and is identical to the signal from the first Hall-sensor but with an added phase term. We can then use the simple relationship in Equation (2.10) to obtain the amplitude of the signal even when the motor is not rotating but this assumes that we only have a pure sinusoidal signal with no higher harmonics, and this is not the case according to the FEA simulations.

$$\begin{aligned} S_{out} &= \sqrt{A^2 \cdot \sin^2(\omega t) + A^2 \cdot \sin^2(\omega t + \pi/2)} \\ &= A \cdot \sqrt{sin^2(\omega t) + \cos^2(\omega t)} = A \end{aligned} \tag{2.10}$$

To account for the higher harmonic the expression needs to be reworked and in

Equation (2.11) we obtain an expression for the signal.

$$\begin{aligned} S_{out} &= [S_{Hall1}]^2 + [S_{Hall2}]^2 \\ &= [A\sin(\omega t) + B\sin(3\omega t + \phi)]^2 + [A\cos(\omega t) + B\cos(3\omega t + \phi)]^2 \\ &= A^2 + B^2 + AB\cos(2\omega t + \phi) \end{aligned} \tag{2.11}$$

The amplitude for the first harmonic A ranges from 34 mT to 267 mT, and the third harmonic B ranges from 1.5 mT to 6.6 mT. The amplitude of the third harmonic is small compared to the amplitude of the first harmonic. From the expression we see that the signal consists of a large DC component that is related to the amplitude of the first and third harmonics of the signal. The signal also contains an unwanted ripple with double the frequency as the signal from the Hall-sensors. It is possible to take the square root of the signal since it is always positive since the cosine is limited by ± 1 and $A^2 + B^2 \pm 2AB = (A \pm B)^2 \geq 0$ for all A and B.

Model of dual magnet ring sensor

From the simulation results a relationship between the signal from the Hall-sensors and the input parameters θ_{rel} and the frequency of the motor can be established and A, B and ϕ in Equation (2.9) can be determined. The frequency of the motor only affects the frequency of the signal and the relationship between the frequency of the signal and the motor is described by

$$\omega = N \cdot \omega_{motor} \tag{2.12}$$

where ω is the frequency of the signal from the Hall-sensors, ω_{motor} is the frequency of the motor and N is the number of pole pairs in the magnet rings.

2.2.3 Using the torque sensor for index rotor position

Torque supplied by the rider is not the only physical quantity in an e-bike motor that is of interest. The position of the rotor is needed to control the motor in a satisfactory way. To be able to use the torque sensor geometry to get an index signal for the rotor position could reduce the demands on the rotor position sensor. If the signal from the torque sensor would give an indication when each new electrical period of the motor start, then the position sensor only need to give the position in the electrical period. For example if the position sensor gives 1000 pulses per mechanical revolution but no absolute position, then the torque sensor could be used to establish where each electrical period starts, and possibly simplify the rotor position sensor.

2.3 Demagnetization of NeFeB magnets

The sensor described in Section 2.2.1 uses a magnetic circuit to measure torque. The strength of the magnet will affect the magnetic flux density in the sensor and when measuring with a Hall-sensor the flux need to be kept in the range of the sensor. It is possible to decrease the strength of a permanent NeFeB magnet by heating it. The decrease in strength is dependent on the permeance coefficient or the load line for the magnet and the grade of the magnet. The magnet used in this project is grade N42 and the permeance coefficient depends on the geometry of the magnet. For the magnet used in the prototype sensor described in Section 3.4 the permeance coefficient is 0.15 [9]. The demagnetization curve

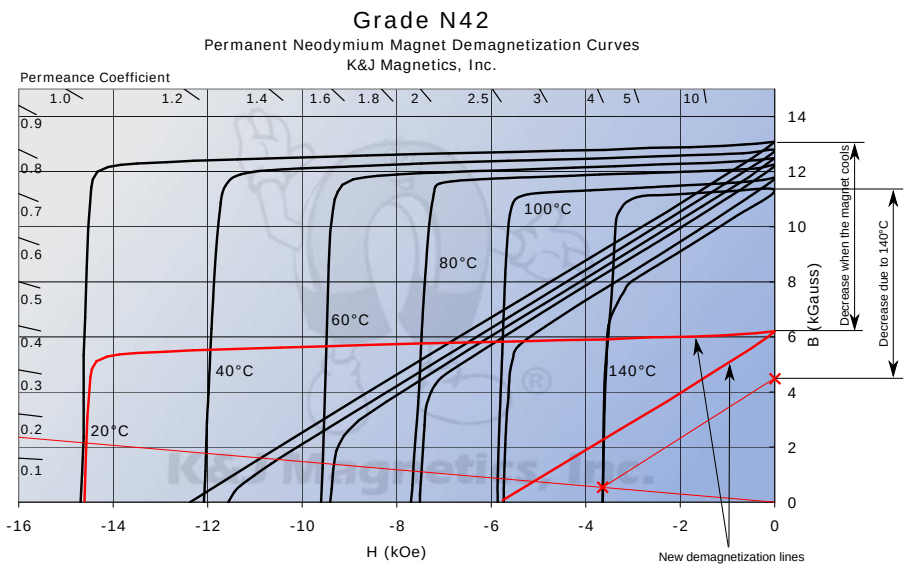

Figure 2.18: Demagnetization curve for N42 NdFeB magnets [10].

for a magnet is dependent on the temperature. To calculate how much strength the magnet will lose for a certain temperature a guide from [10] is used. To get the loss due to high temperature you first check where the load line (permeance

coefficient) cross the curve for the temperature you are interested in. From the intersection you draw a line parallel to the temperature line to the axis on the left. The distance between the crossing of the axis and the line and to the original crossing of the axis at room temperature is the amount you should shift the whole curve downwards to get the resulting demagnetization curve. Figure 2.18 illustrates the estimation of the shift in the demagnetization curve due to high temperatures. If the magnet is brought up to the same temperature again it will not degrade any further [10]. If the strength of the magnet after heating is still too high the temperature can be raised additionally to reduce the strength further. When the magnet is heated to its curie temperature the magnet loses all of its strength. For NdFeB N42 the curie temperature is 310 °C [10].

2.4 Currently used sensors

In this section a brief overview of the torque sensors currently used for Höganäs e-bikes is given. The sensors are a ready-made components that Höganäs buy from the manufacturer of each sensor. The two sensors are not integrated in the motor and measure torque on different parts of the bike.

2.4.1 ID bike TMM4

The torque sensor TMM4 from IDbike is mounted on the right rear dropout. The dropout is where the back wheel is attached. The sensor has a structure that deforms when torque is applied to the chain. The deformation is measured with a Hall-sensor and a magnet and is proportional to applied torque. In Figure 2.19 the TMM4 torque sensor is depicted. The frame of the bike needs to be modified when TMM4 is used to fit the sensor.

2.4.2 Thun X-Cell RT

The torque sensor from Thun [12] model X-cell RT is mounted in the bottom bracket and the pedals are then attached to the axle of the sensor. When torque is applied by the rider to the left pedal there will be a slight torsion of the axle. The axle is made from a magnetostrictive material [13] with two magnetized patters on it. The torsion of the axle will give a change in the magnetic field from the magnetized patterns as described in Section 2.1.5. The two patterns are magnetized with opposite direction and the magnetic fields are read with coils with high sensitivity. The sensor also has a magnetized pattern for sensing rotation. A downside with this sensor is that it only registers torque applied to

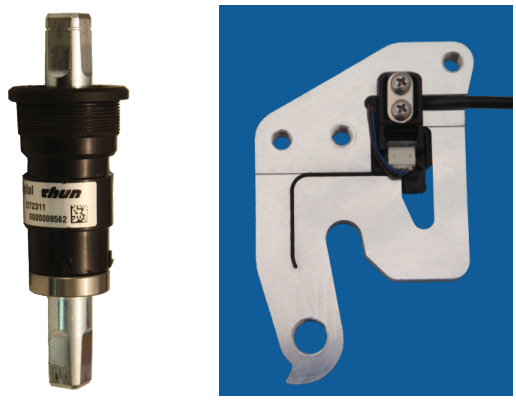

Figure 2.19: The torque sensors used with Höganäs e-bike motor. To the left X-cell RT from Thun and to the right TMM4 from IDbike. The image of TMM4 is copied from [11].

the left pedal since torque applied to the right pedal will be applied directly to the chain and not cause a torsion of the axle.

3 Method

3.1 Investigation of competitors' solutions

Höganäs has bought e-bike motors from some of its competitors to study how the competitors have solved the problem of integrating a torque sensor in their motor. The motors are disassembled and studied. Since all the motors are different the disassembly procedure is different in each case and hard to describe in detail. The actual work is performed by a technician at Höganäs. The work is documented by Höganäs and only the study of the torque sensor is considered in this report.

3.2 FEA of magnetic based torque sensors

To get an understanding on how a magnetic based torque sensors work they are simulated in a finite element analysis (FEA) program. The program used is JMag and is developed by JSOL Corporation. The program is specialized for electromechanical simulations. The program outputs among other things the magnetic flux density for the simulated sensor. The program can simulate both static scenarios and transient scenarios where parts of the sensor move.

3.2.1 CAD-model of sensor

To simulate a sensor in JMag the geometry of the sensor needs to be modeled. The modeling is done with CAD software where the geometry is defined. The software used for generating models in this project is Solid Works. To investigate how the different parameters of the geometry affect the sensor different sensor models are simulated.

3.2.2 Meshing the model

Once the geometry for the sensor has been modeled it needs to be divided into small segments. This procedure is called meshing. The number of elements will greatly affect the computation time for the simulation. If the element size is reduced the number of elements will increase for the same model.

The element size will also affect the quality of the result. A finer mesh will give more accurate result but the size of the mesh needs to be put in relation to

the smallest detail in the model. Regions that are especially interesting should have a finer mesh to increase the quality of the result and regions that are of less interest should have a course mesh to save calculation time.

3.2.3 Defining boundary conditions

Before simulating a number of conditions need to be defined for the simulation. For example the materials used in the model should be defined. Moving parts in the sensor are also defined as a boundary condition. If the simulation uses symmetry in the model to reduce calculation time then this should be defined as a boundary condition.

3.2.4 Extracting results

Since FEM programs are designed to simulate a variety of scenarios they will not automatically output the information you want. To study for example the magnetic flux density in an air gap you need to define a line in the center of the air gap and the program will calculate the magnetic flux density along this line. The FEA program has a wide variety of functions that you can apply to your results. The program can also generate vector plots, line plots and contour plots to illustrate the simulated result.

3.3 Simulink models of sensor

To study the signal from the simulated sensor described in Section 2.2.2 it is modeled in Simulation program Simulink that is a part of Matlab. The model will produce a signal as a function of the parameters frequency of the motor and relative rotation between the two magnet rings. It is also possible to study the effect of misplacement of the Hall-sensors by introducing a small delay in one of the signals. The signals from the models can be used to design filters and to study different scenarios that might arise when the sensor is used.

3.4 Prototype of torque sensor

To ensure that the magnetic based torque sensor work in real life and not only in the simulation a prototype needs to be built and evaluated. The prototype consists of a magnetic circuit that changes reluctance when a part of it is rotated. The prototype is not tested in the motor that it is intended to be built into. This is to simplify the prototype since the dimensions of the motor and

the magnetic disturbance in the motor does not need to be considered. To further simplify the prototype the mechanical device that converts the applied torque to a rotation is not included. Instead one part of the sensor is slowly rotated and the magnetic flux density is measured in the air gap. To get a precise measurement the position of the inner part of the sensor the position is measured with a rotary encoder as it is turned. The flux density in the air gap is measured with an analog Hall-sensor connected to voltage measurement module in a FPGA system from National Instruments. The rotary encoder is connected to a digital module in the FPGA. The data from the FPGA system is acquired with LabView and exported to Matlab for plotting purposes. The equipment used for the measurement is listed in Table 3.1 and in Figure 3.1 the measurement setup is depicted. Normally this setup is used to measure cogging torque in motors and the dimensions of the prototype sensor are adapted to fit the measurement rig. The dimensions of the prototype are also adapted to fit a ready-made magnet ring to avoid ordering a custom made magnet ring since it generally requires that you order large quantities when ordering custom size magnets. The magnet used in the prototype has dimensions outer diameter: 101 mm, inner diameter: 60 mm and thickness: 4 mm. These dimensions are far greater than what is suitable to integrate in Höganäs e-bike motor but it will still work to evaluate if the concept works. Since the dimensions are changed new simulations are done with the same dimensions as the prototype. This is done so that the simulated result and the measured result can be compared. In Appendix A the drawings for manufacturing the prototype sensor are included.

Equipment	**Model**
Planetary Servo Gearbox	Wittenstein alphira® 060
FPGA	NI 9164
Voltage-module	NI 9239
Digital-module	SEA cRIO EN Dat
Rotary encoder	Heidenhain ECN 125 2048 1SS08-C4
Hall-sensor	Allegro Microsystems A1302KUA-T
Power supply	IT *i* EL302R Power supply 30V2A

Table 3.1: Equipment used for evaluating the changing reluctance single magnet torque sensor.

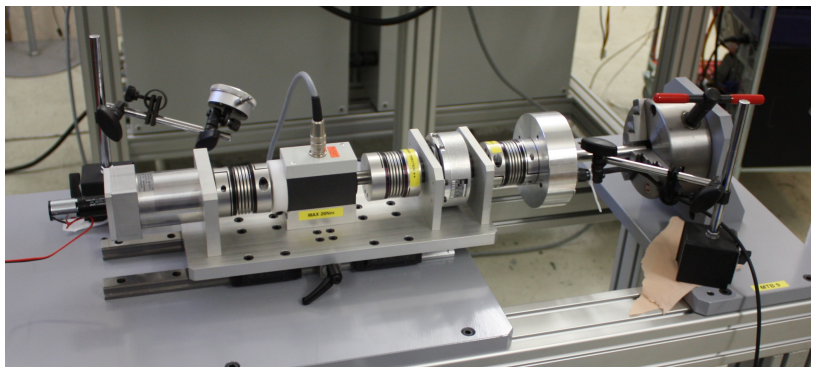

Figure 3.1: Measurement setup used to evaluate the prototype sensor.

3.4.1 Measuring magnetic flux density in Höganäs motor

Electric motors generate magnetic fields that when measuring torque with the help of a magnetic circuit is considered noise. The current in the windings and the permanent magnets produce magnetic fields that may interfere with the measurements. To get an understanding of how large the interferences are a Hall-sensor is placed inside the motor. The sensor is placed between two iron pieces to emulate the conditions for the sensor prototype described in Section 2.2.1. The two iron pieces will shield the Hall-sensor partially a in the case with the prototype sensor. The signal cable used to connect the Hall-sensor is located right next to the power cables and to minimize disturbances not caused by the magnetic fields in the motor a shielded cable is used.

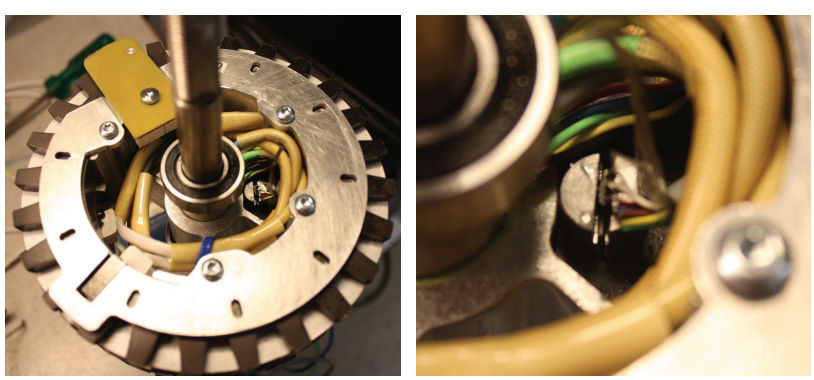

Figure 3.2: The Hall-sensor placed in the motor for measuring magnetic disturbances.

4 Results

4.1 Competitors' solutions

4.1.1 BionX torque sensor

The e-bike motor from BionX is equipped with a strain gauge on the back axle see Figure 4.1. The strain gauge measure the bend of the axle caused by the torque applied by the rider. The strain gauge in covered with a protective coating since metal foil strain gauges are fragile. The solution is simple but requires electronics close to the sensor to amplify the signal since the signal from the sensor is very weak.

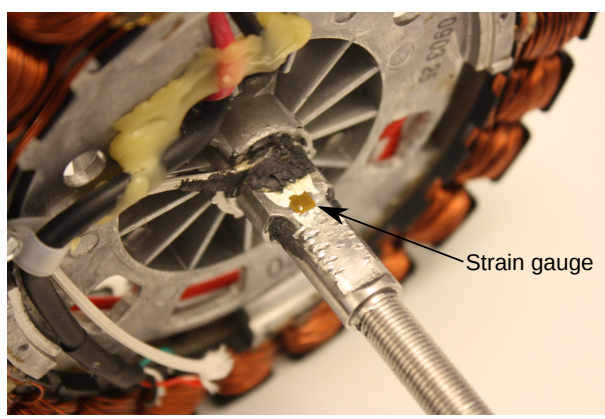

Figure 4.1: The torque sensor in the BionX motor.

4.1.2 GO SwissDrive torque sensor

The torque sensor for the GO SwissDrive is a magnetic circuit that scans a multi-pole magnetic ring. The resulting magnetic flux density is measured with an analog Hall-sensor. The Hall-sensor gives a voltage proportional to the magnetic flux density as described in Section 2.1.6. On the inner part of the sensor there are a number of protruding teeth that are facing the magnetic poles on the outer ring. When the inner part is rotated the teeth are shifted from a magnet with magnetization inwards to a magnet with magnetization outward giving a

magnetic flux density in the air gap where the Hall-sensor is located that depends on how the teeth are aligned with the magnet ring. The sensor is equipped with a rubber bushing to get a turning that is proportional to applied torque an it is also equipped with a mechanical stop to prevent permanent deformation of the rubber bushing. The downside with this technique is that extra ball bearings are needed and the lifetime of the rubber needs to be investigated. Temperature variations will probably affect the rubber bushings stiffness giving a change in measured value. Appealing properties of this technique are that

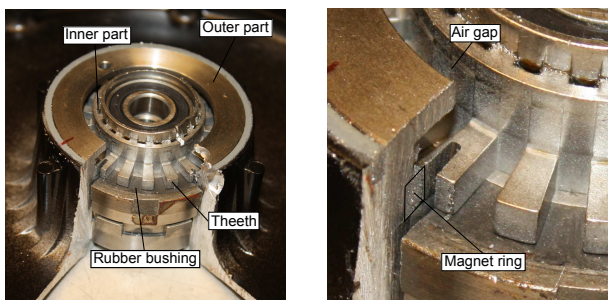

Figure 4.2: The torque sensor of the GO SwissDrive

it gives a continuous reading of the applied torque and it does not require the wheels of the bicycle to move to get a measurement. In Figure 4.2 the torque sensor in the GO SwissDrive is depicted and in Figure 4.3 the magnetic circuit of the GO SwissDrive torque sensor is illustrated.

FEA analysis of GO SwissDrive torque sensor

To get an understanding for how the GO SwissDrive torque sensor works in detail the sensor was modeled and simulated in the FEA program JMag. Since the material used in the sensor and the type of magnet used is unknown the result can only be used to see the general principle of the sensor. The actual values for the different physical quantities do not correspond in magnitude to those in the actual sensor. In Figure 4.4 the magnetic flux density from the simulated sensor is depicted. The figure shows the result when the inner part of the sensor is rotated. The rotation is done in steps of 1 degree and here only every third step is shown. From the simulation result it is clear that the magnetic flux density in the air gap (light gray in the figure) changes as the inner part is rotated. Only 1/20 of the sensor in needed to simulate the senor since it is possible to use the rotational symmetry when computing the simulation to reduce computation time.

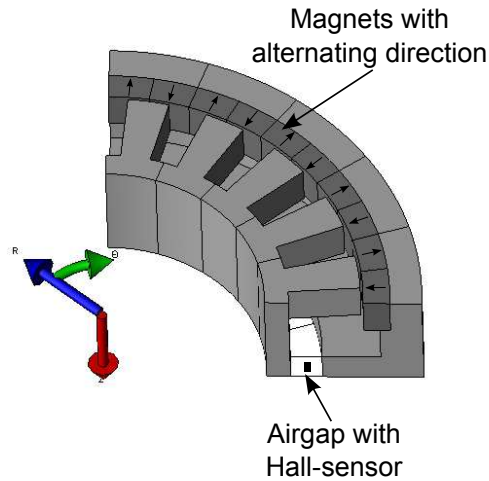

Figure 4.3: The magnetic circuit of the torque sensor in the GO SwissDrive motor with coordinate system.

To get a more accurate measure on how the magnetic flux density varies as torque is applied the average magnetic flux density in radial direction in the air gap was calculated. The radial direction is towards the center of the sensor and is the magnetic flux density that a Hall-sensor placed in the air gap would measure. The relationship depicted in the figure is not the relationship between torque and output voltage from the Hall-sensor, but the relationship between rotation and the magnetic flux density in the air gap. To get the relationship between torque and output voltage the rubber bushings relationship between applied torque and rotation should to be added to the model. The sensitivity of the Hall-sensor used should also be considered as it will scale the output signal.

It is possible to choose where on the rotation-magnetic flux density curve the sensor should operate, and to get a nice linear relationship between magnetic flux density and rotation the sensor should work in the linear region around the zero crossing. Figure 4.5 show the magnetic flux density at different rotation angles. Since the whole sensor is rotating when the back wheel of the bike turns it is important to know how the signal from the torque sensor changes as it rotates. To measure the magnetic flux density in the air gap when the sensor turns a circle was defined in the air gap and the FEA program calculated the magnetic flux density along this line. In Figure 4.6 the resulting magnetic flux density is plotted when the sensor rotates. The plot shows several lines that correspond to how much the inner part has been rotated. It is clear that we see very little variation when the sensor rotates, and this is because there are

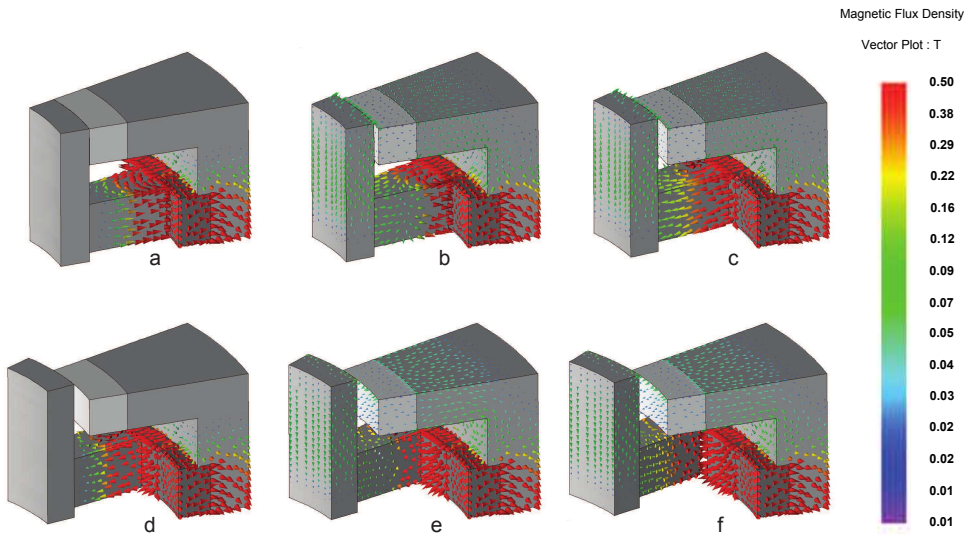

Figure 4.4: Simulation result of the torque sensor in the GoSwiss Drive motor. (note:logarithmic scale).

a large amount of magnets giving a symmetric field in the rotation direction. This symmetry means that no signal processing needs to be performed and the signal only depends on the applied torque.

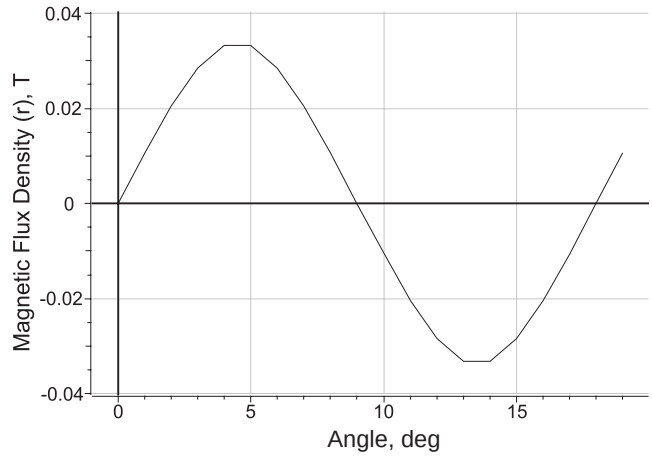

Figure 4.5: Simulated magnetic flux density in radial direction in the air gap.

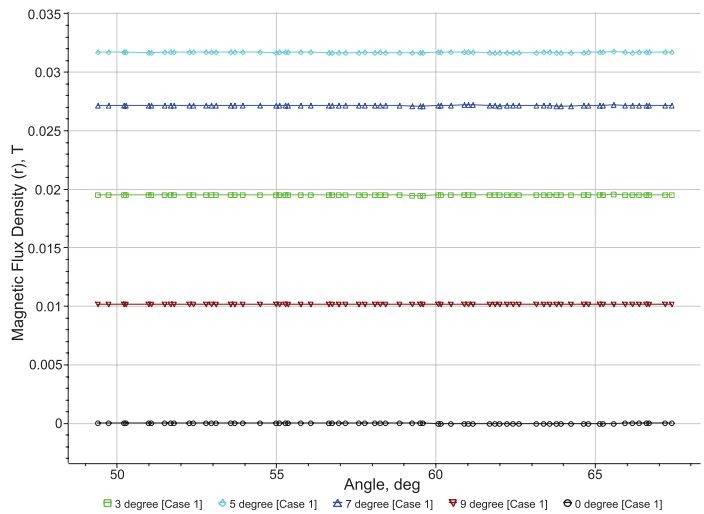

Figure 4.6: Simulated magnetic flux density in radial direction when moving the sensor in circular direction in the air gap.

4.1.3 Xion motor torque sensor

In the Xion motor there is a high resolution reflective optical position encoder (model AEDR-8502-102 [14] or similar) that gives the rotor position with high accuracy and the torque is measured by comparing the position of a flexible inner part to the position of the rotor. The position of the flexible inner part is measured with a multipole magnetic ring and two Hall-sensors. Figure 4.7 depict the magnet ring and the reflective tape in the motor and Figure 4.8 depicts the two Hall-sensors and the reflective position encoder.

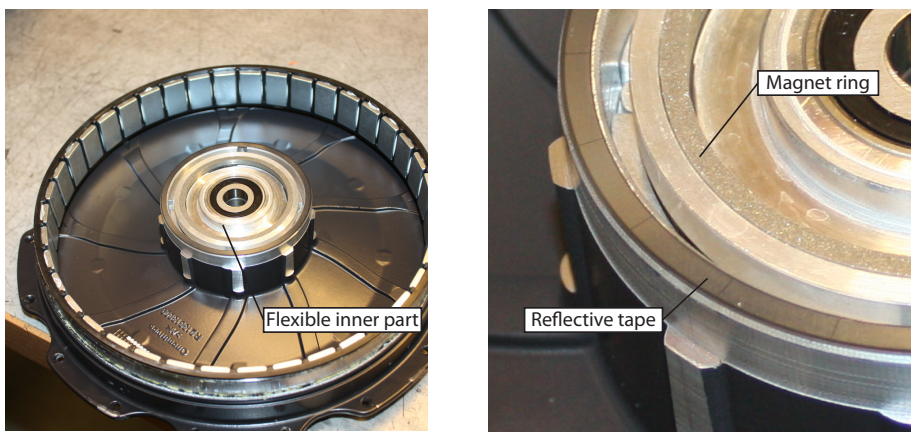

Figure 4.7: The magnetic ring and reflective tape in the Xion motor.

The flexible coupling between the inner and the outer part is achieved with mechanical springs see Figure 4.9. There is also a mechanical stop to prevent the springs from compressing more than they can handle to prevent damage to the springs. The optical sensor is sensitive to high temperature and can withstand maximum 85 °C [14] and limits the maximum temperature in the motor if this type of sensor is used in Höganäs e-bike motor.

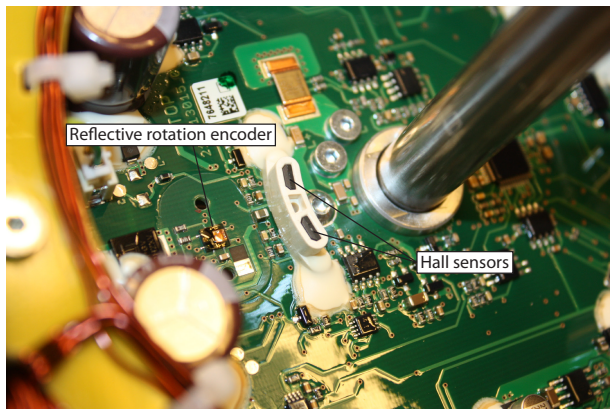

Figure 4.8: The two Hall-sensors in a plastic hold and the reflective rotation encoder.

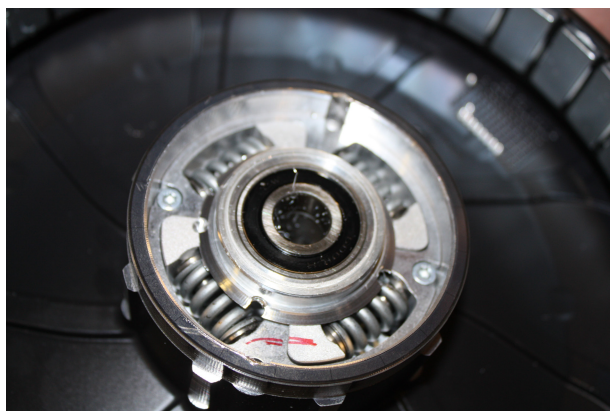

Figure 4.9: The inner part with the magnet ring removed to expose the mechanical springs that give a flexible coupling between the inner part and the rotor.

4.2 Specifications torque sensor

Below is a list of properties that you want to have in an integrated torque sensor. It is not probable that all of these criteria can be fulfilled at once and you have to make a trade of between the different properties. Some of the properties can be achieved or improved with the help of signal processing and electronics.

- Withstand temperatures up to 120 °C with no temperature drift.
- Measure torque on the interval 0 N m to 200 N m and withstand up to 600 N m without permanent damage to the sensor.
- The sensor should have a stable zero level.
- The sensor should be insensitive to disturbances from the motors magnetic fields.
- It should be robust and insensitive to mechanical disturbances caused by the rider.
- The sensor should have an adequate number of measuring points if the sensor is discrete sensor (measuring only at certain point in time or space).
- If it is required that the wheel turns to get a reading of the torque the angle needed should be small.
- If the sensor needs electronics inside the motor they need to withstand the magnetic fields and the high temperature in the motor.
- The sensor should have a well-defined output signal with a well-known relationship between the applied torque and output signal.
- The signal should not be interfered when it is transmitted to the motor control unit.
- The sensor should preferable not rotate with the motor. If the sensor rotated it should be able to transmit the information to the non-rotating part of the motor.
- It should be possible to fit the torque sensor inside the e-bike motor.

4.3 Changing reluctance single magnet sensor

4.3.1 FEA simulation of the magnetic circuit

The result from the initial simulations to see if it is possible to design a torque sensor with one magnet ring and a structure with changing reluctance as described in Section 2.2.1 to measure torque is plotted in Figure 4.10. The result shows that the magnetic flux density will vary in the air gap where the Hall-sensor is located. The signal will vary around an offset that depends on the design of the sensor and the strength of the magnet.

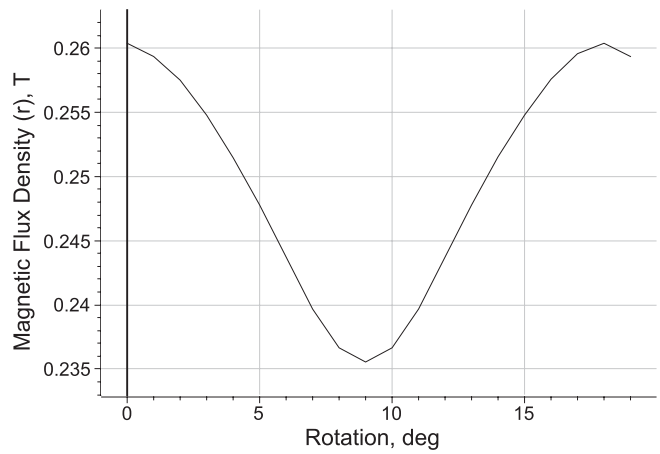

Figure 4.10: Simulated magnetic flux density in radial direction in the air gap.

4.3.2 FEA simulation of the prototype

Since the prototype sensor is built with a ready-made magnet ring with larger dimensions the magnetics of the prototype sensor is simulated again, but with the correct dimensions for the prototype. The simulations show that we get much higher flux density in the air gap, but it is the offset in the signal that increases. The peak to peak value for the signal (the actual value representing the applied torque) is not increased. This is problematic since the signal is measured with a Hall-sensor with a certain maximum output voltage. If the magnetic flux density is too high the Hall-sensor will be saturated. To decrease the flux density the sensor can be rotated or moved out a bit from the air gap, but this will also decrease the amplitude of the torque signal and we would get a signal with lower amplitude. Instead the effect of changing the strength

of the magnet is investigated and in Figure 4.11 the magnetic flux density in the air gap is plotted for different strength of the magnet. The strength of the magnet is reduced from 100% down to 20% in steps of 20%. The offset in the signal is significantly reduced and the amplitude of the torque signal is affected very little. With a lower offset it is possible to use a Hall-sensor with high sensitivity and not saturate the sensor. According to Equation (2.6) we get a max sensitivity for the Hall-sensor with 20% magnet strength ($B_{max} = 0.16\,\mathrm{T}$) of $S = 15.625\,\mathrm{V/T} = 1.5625\,\mathrm{mV/G}$ and a typical Hall-sensor has $S = 1.3\,\mathrm{mV/G}$ to $5\,\mathrm{mV/G}$. The signal from the Hall sensor when using a sensor with $S = 1.3\,\mathrm{mV/G}$ will have an amplitude change of 260 mV that represent zero to max torque.

In Figure 4.12 the simulated magnetic flux density for different distance between the inner and outer teeth are plotted. From the simulation it is clear that the amplitude of the signal can be optimized with regard to the distance. When the distance between the teeth is decreased the magnetic flux density will increase and the Hall-sensor might become saturated. To prevent saturation of the Hall-sensor the magnet size can be decreased.

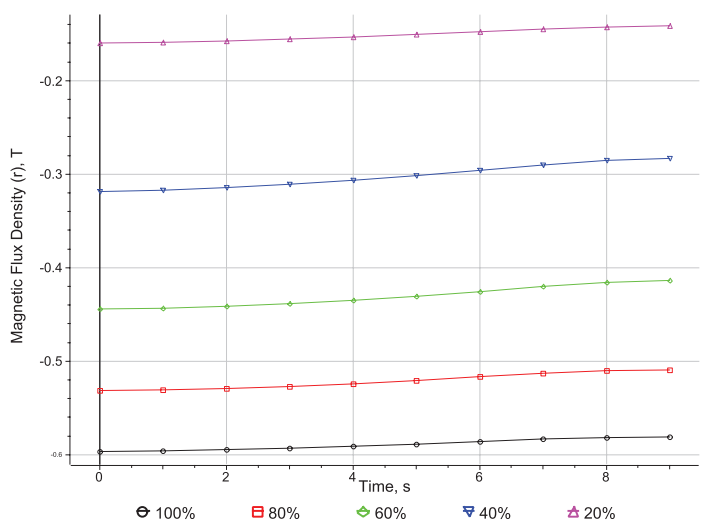

Figure 4.11: Simulated magnetic flux density for the prototype sensor with different magnet strength.

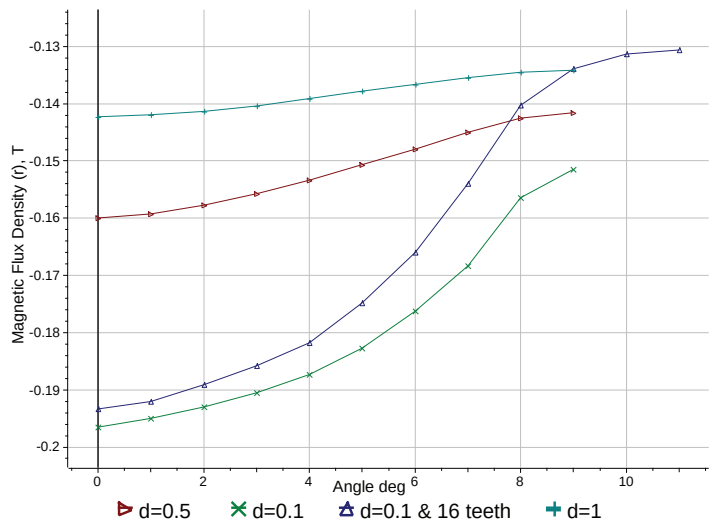

Figure 4.12: Simulated magnetic flux density for the prototype sensor with different gap size between the teeth.

4.3.3 Prototype result

Figure 4.13 depict the prototype sensor. In the right part of the picture the teeth that cause the change in reluctance is shown and in Figure 4.14 the placement of the Hall-sensor in the air-gap is depicted.

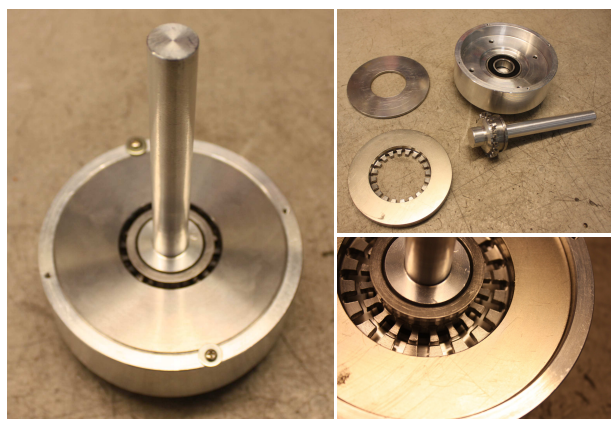

Figure 4.13: The torque sensor prototype of the single magnet changing reluctance sensor.

Figure 4.14: The Hall-sensor placed in the air gap of the torque sensor prototype.

Initial flux measurements

When the sensor is assembled the magnetic flux density in the air gap is measured with a flux meter and is around 0.45 T. This is well outside the range of the Hall-sensor used in the measurements of the prototype. The magnet is heated to 150 °C and the magnetic flux density is measured again. The magnetic flux density is now around 160 mT an can be measured with a Hall-sensor with the sensitivity 13 mV/mT.

Measurement of output signal from the Hall-sensor

In Figure 4.15 the output voltage from the Hall-sensor is plotted. The measured signal amplitude is lower than expected and when the sensor was evaluated it was discovered that the dimensions of the prototype were wrong. The outer diameter of the inner part was wrong, and the air gap between the teeth was increased by approximately 0.5 mm and the total distance was approximately 1 mm. Since the dimensions of the prototype did not correspond with the simulations new simulations were made and in Figure 4.12 the top most line corresponds to an air gap of 1 mm. From the simulations it is clear that an increased air-gap between the teeth gives a lower amplitude for the B-field in the air-gap where the Hall-sensor is located.

The peak to peak value of the measured signal is approximately 85 mV and with the sensitivity of 13 mV/mT corresponds to 6.54 mT peak to peak value compared to 8 mT in the simulation. The offset of the signal in the measurement is 164 mT and the offset in the simulation is 138 mT. The difference in offset is probably caused by difference in magnet strength in the simulation and the prototype.

The sensor is normally turned at most 9° but when the prototype was evaluated the sensor was turned a whole revolution an in Figure 4.16 the signal obtained is plotted. The variation in the signal levels is caused by misalignment of the inner and outer parts of the sensor resulting in a variation in the width of the two air-gaps. When the air-gaps are smaller the amplitude goes up and when its wider the amplitude goes down. Normally both the inner and outer part of the sensor is rotating with a relative rotation between the both parts.

Magnetic flux density in Höganäs motor

The magnetic flux density was measured in the motor as described in Section 3.4.1 and in Figure 4.17 and Figure 4.18 the results from the measurements are plotted. The first plot is when the motor is running at 200 rpm and with

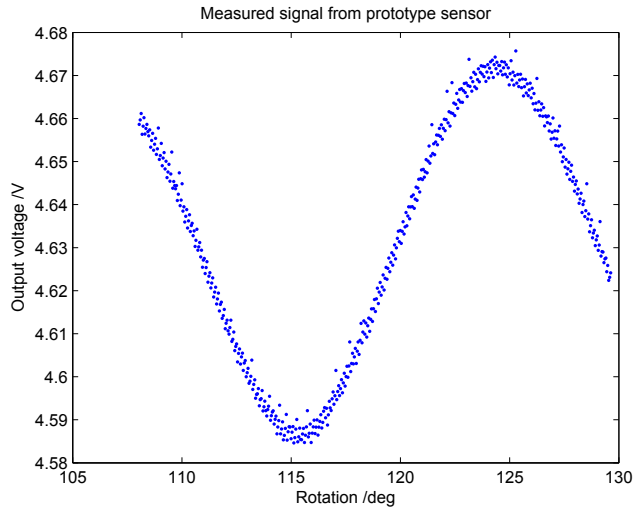

Figure 4.15: Output signal from the Hall-sensor for different rotation angels.

23 N m output torque. In the second plot the motor is running at 80 rpm and the output torque is 40 N m. The disturbances are larger when the output torque is large since a higher current is supplied to the motor which generates a stronger B-field. The largest change in amplitude in the signal from the Hall-sensor due to the disturbances is approximately 0.5 V not considering the fast fluctuation in the signal. This rapid disturbance is caused by the switching in the MCU (motor control unit).

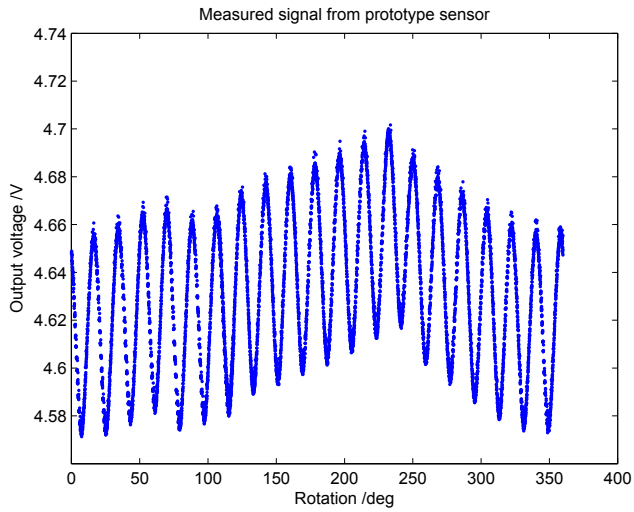

Figure 4.16: Output signal from the Hall-sensor when rotating a whole revolution.

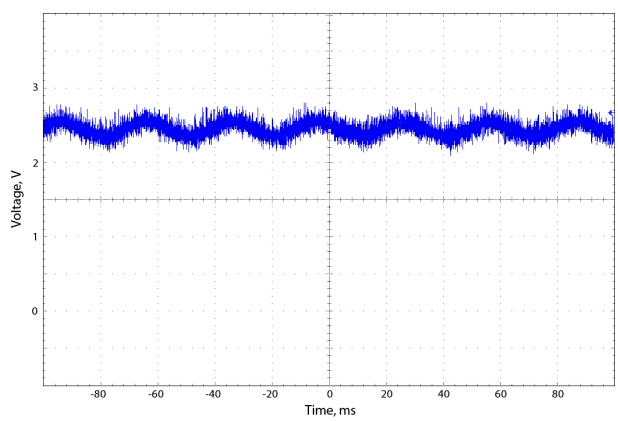

Figure 4.17: The measured disturbances from the motor with 23 N m output torque and 200 rpm.

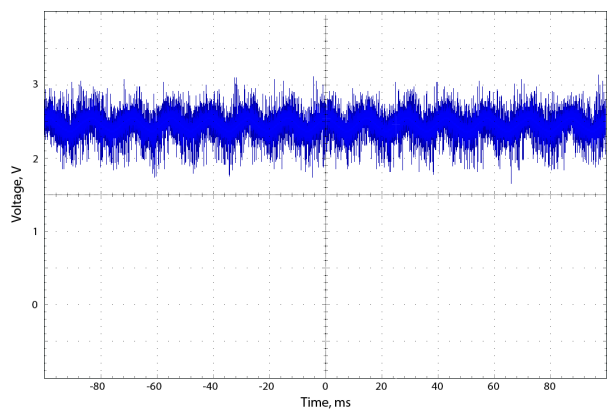

Figure 4.18: The measured disturbances from the motor with 40 N m output torque and 80 rpm.

4.4 Dual magnet ring sensor

From the simulations of the dual magnet ring sensor a Simulink model was created. A print out of the model is added in Appendix B. From the model the output signal from the dual magnet torque sensor is obtained and in Figure 4.19 the output signal has been plotted. The plot also contains the signal from the Hall-sensor and a filtered version of the output signal. The bottom plot is the relative rotation between the magnet rings that corresponds to the applied torque.

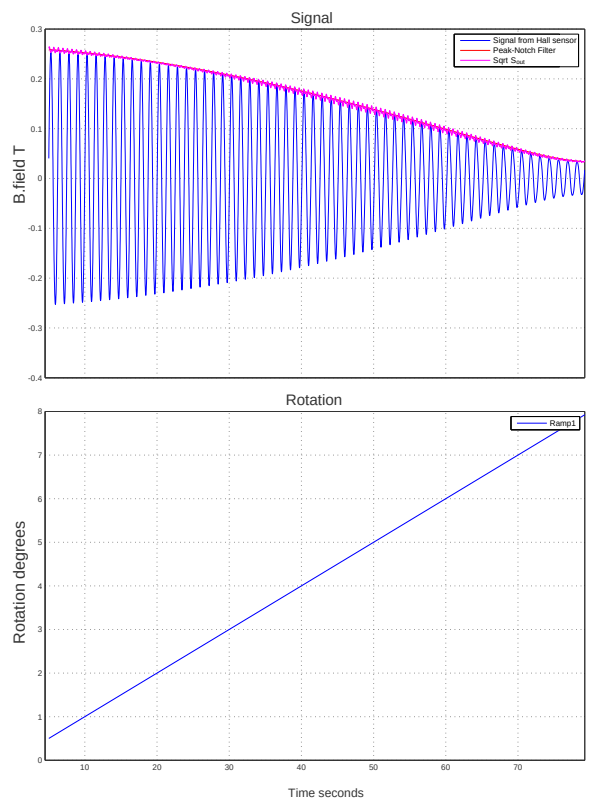

Figure 4.19: Output signal from Simulink model for the dual magnet rings torque sensor.

4.4.1 Sensitivity to geometrical errors

When a sensor is manufactured and mounted in a motor it is virtually impossible to get a sensor without errors. The sensor is manufactured and mounted with a specific tolerance and to investigate the effects of this imperfect manufacturing and mounting of the magnet rings the sensor is simulated with a shift of the center of one of the magnet rings. This shift will cause the rings to be non-concentric and the shift is 0.1 mm. In Figure 4.20 the magnetic flux density between the magnet rings is plotted. There is a large modulation of the peak to peak value of the signal and we get higher amplitude when the air gap is smaller and a lower amplitude on the side where the air gap is smaller.

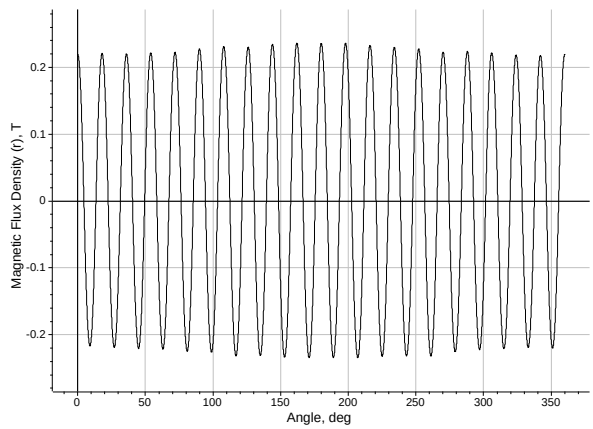

Figure 4.20: The magnetic flux density with a 0.1 mm shift of the center of one of the magnet rings.

5 Discussion

5.1 Limitations due to patents

The development of an integrated torque sensor for Höganäs e-bike motor is limited by the patents held by competitive motor manufacturers. Two types of technologies are discussed to evaluate how they are limited by patents held by competing companies.

5.1.1 Patent No. CA 2,426,109

The patent CA 2,426,109 [15] is a patent for measuring torque by measuring the deformation of the back axle in an e-bike. This patent limits the use of any kind of measuring technology as long as you measure the deformation of the back axle to get a reading of the applied torque. The patent applies specifically to e-bikes and therefor it is not possible for Höganäs to use any technologies that measure torque by measuring the bending of the rear axle.

5.1.2 Patent No. US 4,784,002

The patent US 4,784,002 [16] is a patent for a device that measure difference angle by measuring magnetic flux density. The device uses multiple magnets and a rotor that scans the magnets to get a change in magnetic flux density when torque is applied. The patent is no longer valid and will not limit Höganäs use of this type of technology.

5.1.3 Patent No. US 6,598,490

The patent US 6,598,490 [17] "Apparatus for contact-less measuring the value of a difference angle between two parts rotating about a common axis" is for a similar device described in [16] and one of the key differences is that the magnets are moved together. The device has a rotor that scan the magnets causing a magnetic flux density that varies in strength and direction depending on how the rotor is positioned. The torque sensor in the GO SwissDrive motor described in Section 4.1.2 is an realization of this patent. The device uses a minimum of two magnetic pole pairs which are scanned by the rotor. The prototype sensor evaluated in this project only uses one magnet and works by changing

the reluctance in the sensor to get a change in magnetic flux density. There are many similarities between the prototype developed in this project and the sensor described in this patent but the same applies to the patent US 4,784,002. The properties that distinguish this device from the one described in US 4,784,002 are not used in the prototype developed in this project.

5.2 Evaluated torque sensors

5.2.1 Changing reluctance single magnet sensor

The measurements with prototype sensor gave approximately the same values as the FEA simulations. There is a slight difference in amplitude of the signal but the signal has the same shape as in the simulations. The difference in amplitude can be explained since the strength of the magnet in the simulation is not exactly the same as in reality. The amplitude measured is not good enough but there is room to make several improvements to increase the signal amplitude. For example the distance between the teeth of the inner and outer part can be decreased and the width height ratio of the teeth can be optimized to get the highest possible amplitude.

The sensor requires high mechanical precision when it is manufactured and assembled to ensure that the sensor performs as it is intended. Höganäs motor and MCU (motor control unit) are two separate units and it is not possible to calibrate one MCU to one motor since they are not shipped as a pair. This means that the calibration of the sensor needs to be dynamic and made when the motor and MCU have been connected. Either the calibration is performed by the bicycle manufacturer when the motor and MCU are installed or the calibration is performed automatically during the operation of the motor.

The measurements of magnetic noise in the motor showed that there are magnetic fields from the motor that will interfere with the sensor. The interferences measured are considerably higher in frequency than the torque signal and it should be possible to filter out the majority of the noise. The filter can be placed in the motor on a small PCB. The signal also needs amplification and removal of offset and these operations can also be implemented on the same PCB as the filter.

5.2.2 Dual magnet rings

The sensor technique suggested in Section 2.2.2 is hard to implement outside of the lab. It is hard to get the placement of the magnet rings correct and a

small misalignment will give a large error in the torque signal. Furthermore the orientation of the magnet is hard to ensure. If one of the magnet rings is rotated the amplitude of the signal will be affected and the sensor will give a incorrect reading. The placement of the two Hall-sensors is also important and especially the difference in angle must correspond to a 90° shift in the signal. The overall orientation of the Hall-sensors will also affect the amplitude of the signal since they will only be affected by the magnetic flux density that is in the normal direction to the Hall-sensor. The signal from the sensor will contain a harmonic that needs to be filtered out and the frequency of this harmonic will depend on the speed of the motor and will complicate the filtering since it is not static.

The sensor technique with the dual magnet rings can probably be realized in a lab environment but it is not likely that it will work well as a series produced sensor since it is sensitive to geometrical errors.

5.3 Future goals

There are several tasks remaining in the development of a working torque sensor for Höganäs e-bike motor. For the sensor using a single magnet and changing reluctance the dimensions of the sensor need to be changed to fit the sensor inside the motor. When the dimensions are changed they also need to be optimized to get a good signal. The magnetic flux density should be in the range of what the Hall-sensor can measure and the noise generated by the motor must be considered so that the Hall-sensor will not saturate.

The flexible coupling between the inner and outer parts of the sensor needs to be designed and evaluated. Once the dimensions are established the effects of misalignment and tolerances in the manufacturing of the sensor needs to be investigated. Neodymium magnets are temperature dependent and the strength of the magnet decreases with increased temperature. When the magnet strength changes the magnetic flux density also change and the output signal from the torque sensor changes. The sensor needs to be characterized to be able to compensate for the temperature variations in the motor.

The filter and amplification needed to get a good signal should be designed and tested. The relationship between applied torque and output signal needs to be established and if needed linearized. The control algorithms in the MCU should be reworked to work with the torque sensor.

6 Bibliography

[1] L. Grahm, H. G. Jubrink, and A. Lauber, *Modern industriell mätteknik : givare / Lennart Grahm, Hans-Gunnar Jubrink, Alexander Lauber.* Lund : Teknikinformation ; Studentlitteratur [distributor], 2007 (Lund : KFS), 2007.

[2] T. Kenny, W. Kester, and G. C. Low, "Chapter 19 - strain gages," in *Sensor Technology Handbook* (J. S. Wilson, ed.), pp. 501 – 529, Burlington: Newnes, 1 ed., 2005.

[3] T. M. Adams and R. A. Layton, "Piezoresistive transducers.," *Introductory Mems*, p. 211, 2010.

[4] T. Sachs, R. Grossmann, J. Michel, and E. Schrufer, "Remote sensing using quartz sensors.," in *Proceedings of the SPIE - The International Society for Optical Engineering*, vol. 2718, (Lehrstuhl fur Elektrische Messtechnik, Tech. Univ. Munchen, Germany), pp. 47 – 58, 1996.

[5] P. Blanchard, J. Burnett, G. Erry, A. Greenaway, P. Harrison, B. Mangan, J. Knight, P. Russell, M. Gander, R. McBride, and J. Jones, "Two-dimensional bend sensing with a single, multi-core optical fibre.," *Smart Materials and Structures*, vol. 9, no. 2, pp. 132–140, 2000.

[6] H. Zumbahlen, "Chapter 3 - sensors," in *Linear Circuit Design Handbook* (H. Zumbahlen, ed.), pp. 193 – 243, Burlington: Newnes, 1 ed., 2008.

[7] F. T. Calkins, A. B. Flatau, and M. J. Dapino, "Overview of magnetostrictive sensor technology.," *Journal of Intelligent Material Systems & Structures*, vol. 18, no. 10, pp. 1057 – 1066, 2007.

[8] E. Ramsden, *Hall-Effect Sensors: Theory and Application.* Elsevier Science, 1 ed., 2011.

[9] "K&J Magnetics, inc." https://www.kjmagnetics.com/calculator.asp, April 2014.

[10] "K&J Magnetics, inc." https://www.kjmagnetics.com/blog.asp?p=temperature-and-neodymium-magnets, April 2014.

[11] http://www.idbike.com/index.php/sensors, May 2014.

[12] http://www.thun.de/en/products/bb-cartridges/x-cell-rt/, May 2014.

[13] "NCTE AG." http://www.ncte.com/en/technology/technology.php, May 2014.

[14] "Avagotech." http://www.avagotech.com, April 2014.

[15] J. Dube, G. Lafond, and B. Quirion, "Method and apparatus for proportionally assisted propulsion," Sept. 7 2010. CA Patent 2,426,109.

[16] S. Io, "Torque sensor," Nov. 15 1988. US Patent 4,784,002.

[17] T. Strothmann, "Apparatus for contact-less measuring the value of a difference angle between two parts rotating about a common axis," July 29 2003. US Patent 6,598,490.

A Drawings for sensor prototype

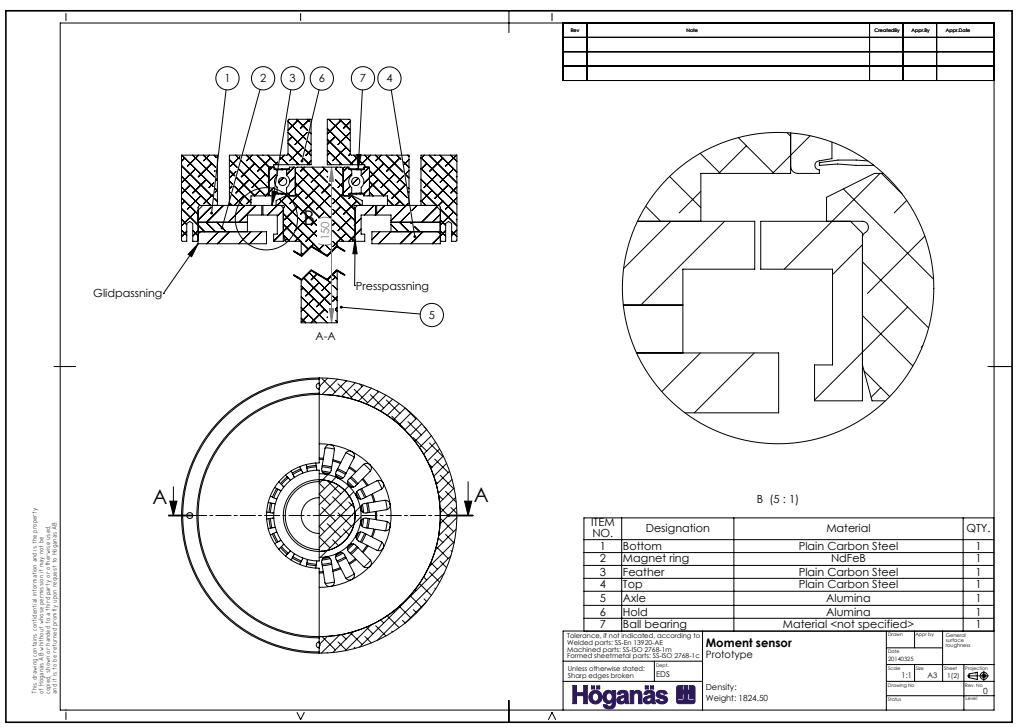

Rev	Note	CreatedBy	Appr.By	Appr.Date

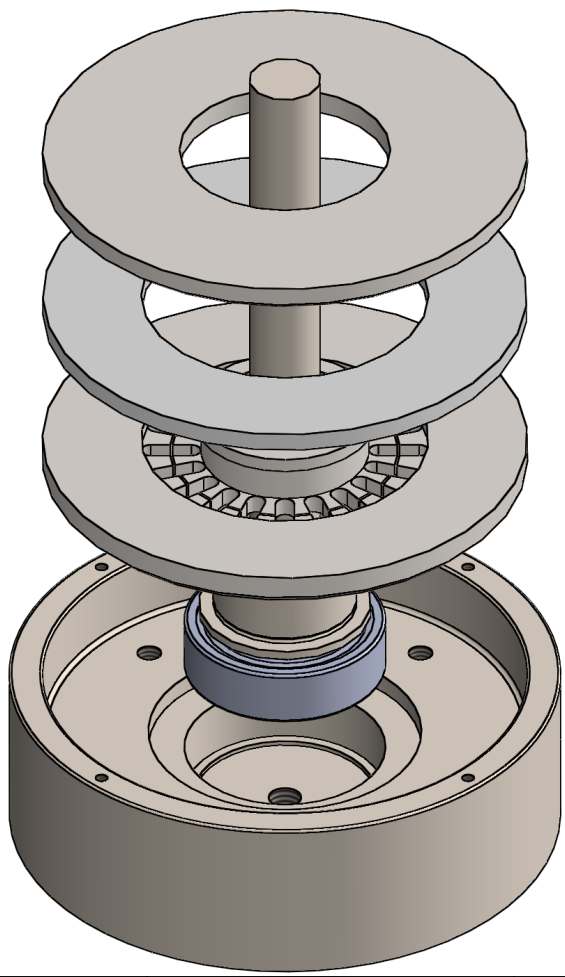

Tolerance, if not indicated, according to
Welded parts: SS-En 13920-AE
Machined parts: SS-ISO 2768-1m
Formed sheetmetal parts: SS-ISO 2768-1c

Unless otherwise stated:
Sharp edges broken

Dept.
EDS

Höganäs

Moment sensor
Prototype

Density:
Weight: 1824.50

Drawn	Appr by	General surface roughness	
Date 20140325			
Scale 1:1	Size A4	Sheet 2(2)	Projection
Drawing No			Rev. No 0
Status			Level

Rev	Note	CreatedBy	Appr.By	Appr.Date

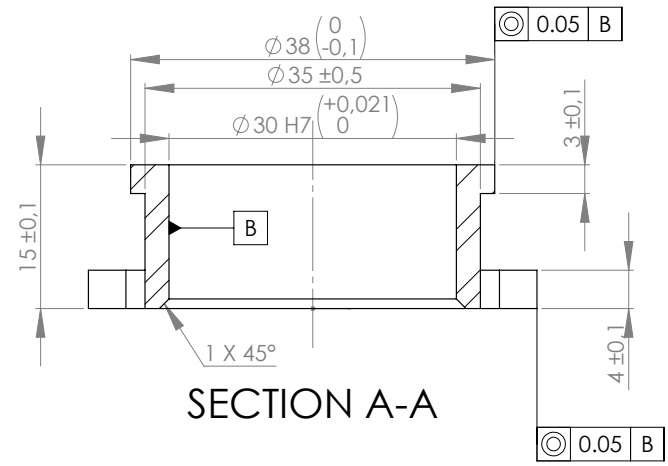

SECTION A-A

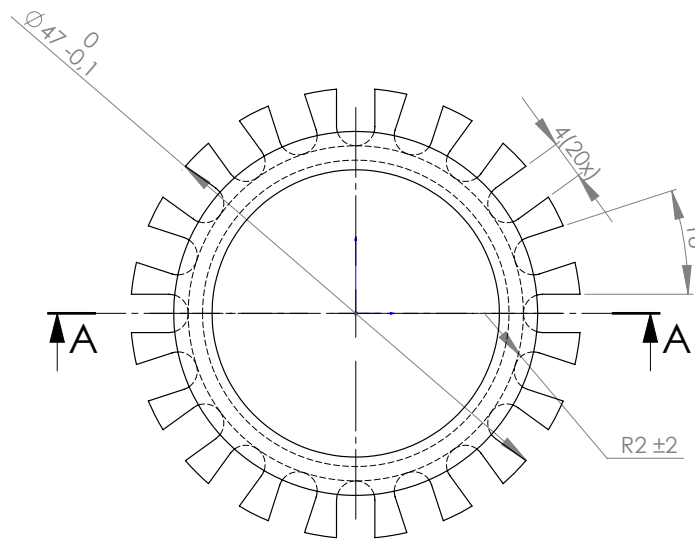

Tolerance, if not indicated, according to
Welded parts: SS-En 13920-AE
Machined parts: SS-ISO 2768-1m
Formed sheetmetal parts: SS-ISO 2768-1c

Unless otherwise stated: Sharp edges broken

Dept. EDS

Höganäs

Feather
Moment sensor prototype

Plain Carbon Steel
Density: 0.0
Weight: 43.8

Drawn	Appr by	General surface roughness
Date 20140325		
Scale 2:1	Size A4	Sheet 1(1) Projection
Drawing No		Rev. No 0
Status		Level

Rev	Note	CreatedBy	Appr.By	Appr.Date

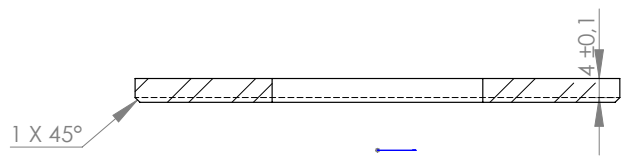

SECTION A-A

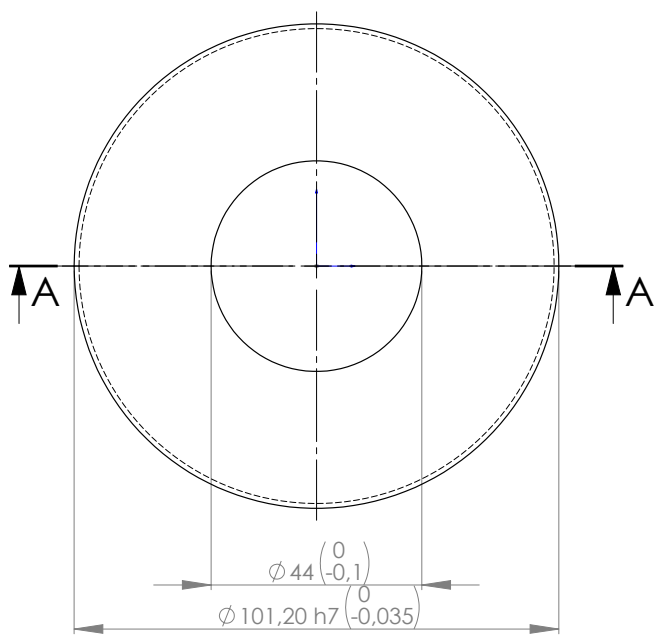

Tolerance, if not indicated, according to
Welded parts: SS-En 13920-AE
Machined parts: SS-ISO 2768-1m
Formed sheetmetal parts: SS-ISO 2768-1c

Unless otherwise stated:
Sharp edges broken

Dept.
EDS

Höganäs

Top
Moment sensor prototype

Plain Carbon Steel
Density:
Weight: 253.2

Drawn	Appr by	General surface roughness
Date 20140325		
Scale 1:1	Size A4	Sheet 1(1)
Projection		
Drawing No		Rev. No 0
Status		Level

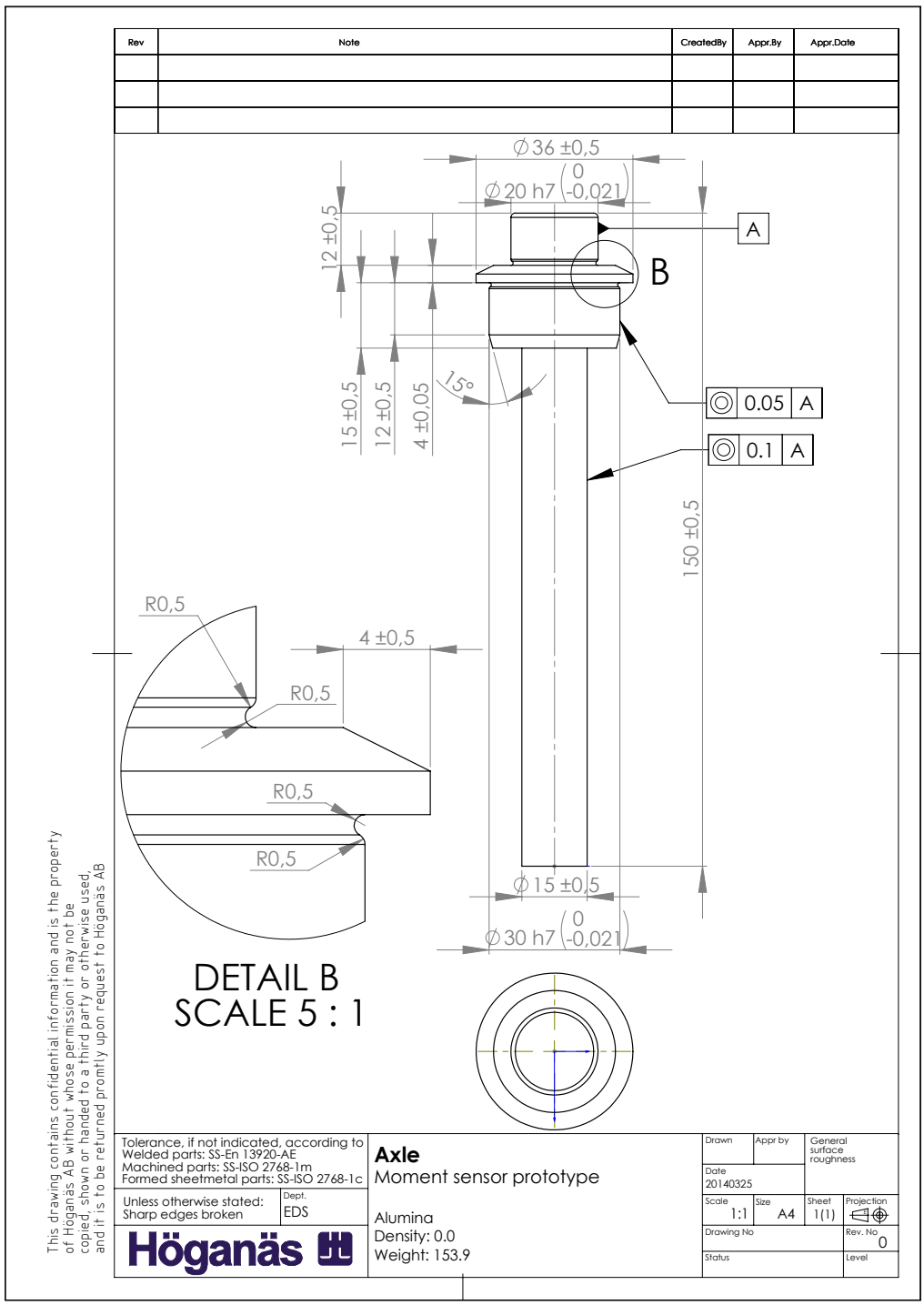
Rev
Note
CreatedBy
Appr.By
Appr.Date
∅36 ±0,5
∅20 h7 (0 -0,021)
12 ±0,5
A
B
15 ±0,5
12 ±0,5
4 ±0,05
15°
0.05 A
0.1 A
150 ±0,5
R0,5
4 ±0,5
R0,5
R0,5
R0,5
∅15 ±0,5
∅30 h7 (0 -0,021)
DETAIL B
SCALE 5 : 1
This drawing contains confidential information and is the property of Höganäs AB without whose permission it may not be copied, shown or handed to a third party or otherwise used, and it is to be returned promtly upon request to Höganäs AB
Tolerance, if not indicated, according to
Welded parts: SS-En 13920-AE
Machined parts: SS-ISO 2768-1m
Formed sheetmetal parts: SS-ISO 2768-1c
Unless otherwise stated:
Sharp edges broken
Dept.
EDS
Höganäs
Axle
Moment sensor prototype
Alumina
Density: 0.0
Weight: 153.9
Drawn
Appr by
General surface roughness
Date
20140325
Scale
1:1
Size
A4
Sheet
1(1)
Projection
Drawing No
Rev. No
0
Status
Level

Rev	Note	CreatedBy	Appr.By	Appr.Date

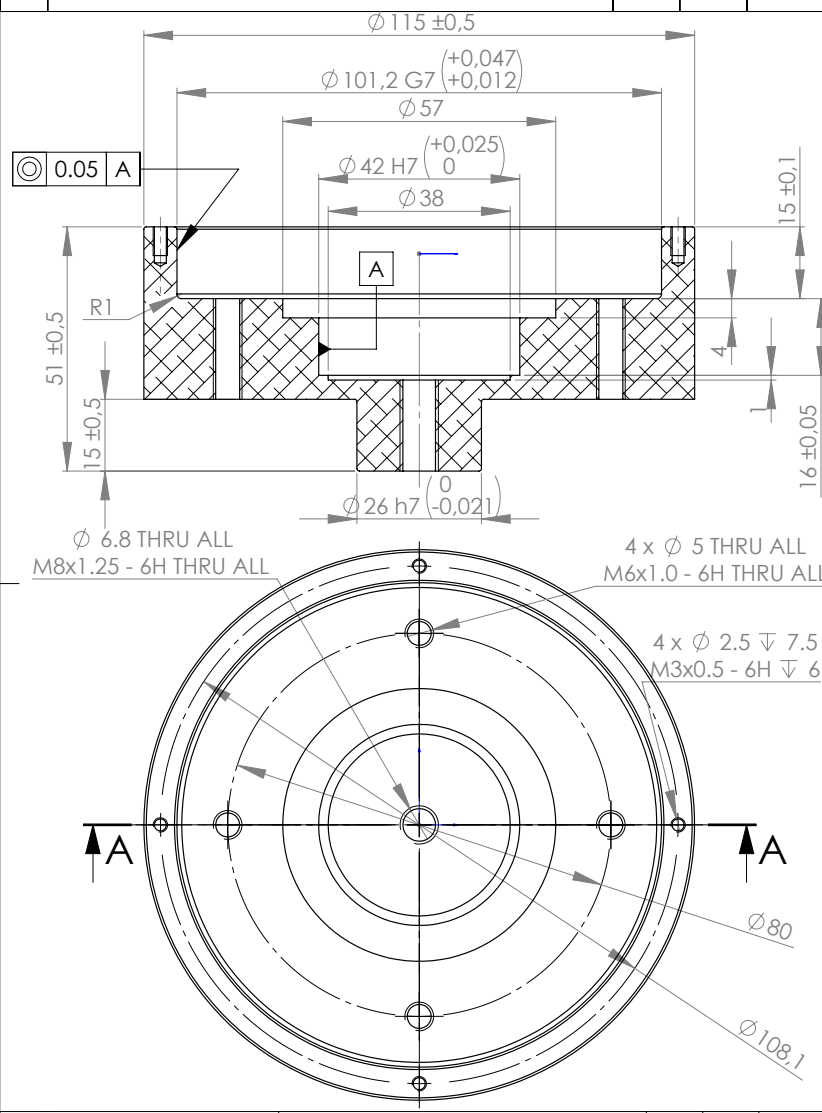

Tolerance, if not indicated, according to
Welded parts: SS-En 13920-AE
Machined parts: SS-ISO 2768-1m
Formed sheetmetal parts: SS-ISO 2768-1c

Unless otherwise stated:
Sharp edges broken

Dept.
EDS

Höganäs

Hold
Moment sensor prototype

Alumina
Density:
Weight: 914.0

Drawn	Appr by	General surface roughness
Date 20140325		
Scale 1:1	Size A4	Sheet 1(1)
Drawing No		Rev. No 0
Status		Level

B Simulink model for dual magnet ring sensor

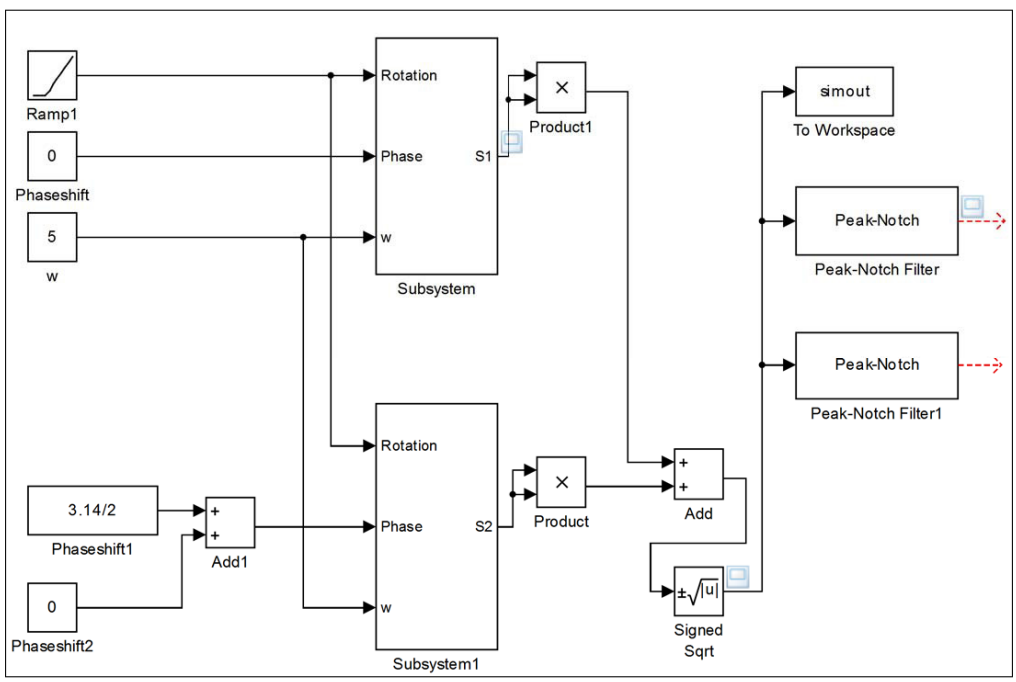

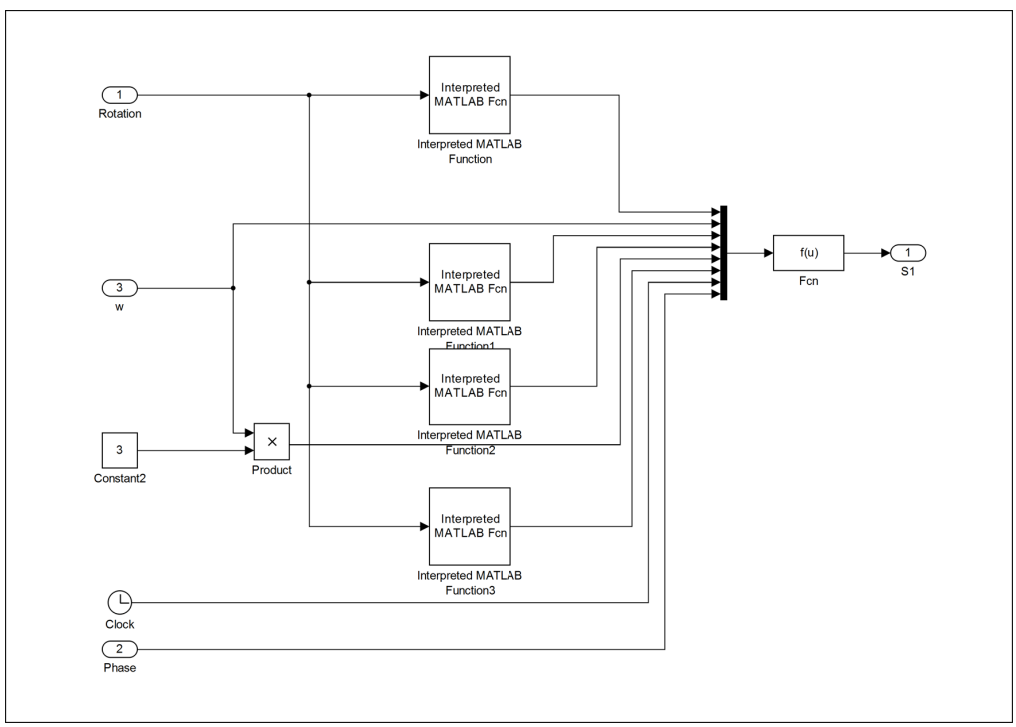
1
Rotation
Interpreted
MATLAB Fcn
Interpreted MATLAB
Function
3
w
Interpreted
MATLAB Fcn
Interpreted MATLAB
Function1
Interpreted
MATLAB Fcn
Interpreted MATLAB
Function2
3
Constant2
×
Product
Interpreted
MATLAB Fcn
Interpreted MATLAB
Function3
f(u)
Fcn
1
S1
Clock
2
Phase